INTERNATIONAL JOURNAL OF INTEGRATED ENGINEERING
ISSN: 2229-838X e-ISSN: 2600-7916

IJIE

Vol. 17 No. 9 (2025) 85-116
https://publisher.uthm.edu.my/ojs/index.php/ijie

Liquid Disintegration Regime of Plain Orifice, Swirl, and Effervescent Atomization: A Review

Zulkifli Abdul Ghaffar[1]*, Salmiah Kasolang[1], Ahmad Hussein Abdul Hamid[1], Rolf D. Reitz[2]

[1] *School of Mechanical Engineering, College of Engineering*
Universiti Teknologi MARA, 40450 Shah Alam, Selangor, MALAYSIA

[2] *Engine Research Center, Engineering Research Building*
1500 Engineering Drive, University of Wisconsin-Madison, Madison, WI 53706 USA

*Corresponding Author: zulkiflighaffar@gmail.com
DOI: https://doi.org/10.30880/ijie.2025.17.09.007

Article Info

Received: 31 April 2025
Accepted: 8 December 2025
Available online: 31 December 2025

Keywords

Liquid disintegration regime, plain orifice atomization, swirl atomization, effervescent atomization, swirl effervescent atomization

Abstract

Liquid atomization is the process by which bulk liquids disintegrate into sprays. Several theories of liquid atomization mechanisms have been proposed to characterize the disintegration process. The liquid disintegration regime map can be used to characterize the process of converting bulk liquid into sprays. This map depicts the steps of liquid disintegration for a liquid atomization process and is a useful tool for understanding the fundamental physics of a given liquid atomization regime. However, a liquid disintegration regime map for a specific form of atomization, swirl effervescent atomization, is currently unavailable and is hypothesized in this research. Swirl effervescent atomization provides numerous benefits in the hybrid category, and it is critical to map the liquid disintegration regime for this type of liquid atomization. The initial step in mapping the liquid disintegration regime is to review the liquid disintegration mechanisms. This article reviews the liquid disintegration regimes of plain orifice, swirl, and effervescent atomization in relation to swirl effervescent atomization.

1. Introduction

Liquid atomization plays a crucial role depending on the application requirements. In a liquid rocket engine, properly designed atomizers ensure efficient and stable combustion. Among the primary purpose of liquid atomization in this application are (i) to increase the surface area of liquid propellant for high combustion efficiency, (ii) to provide nonuniform distributions of mixture ratio and flow intensity, and (iii) to achieve prescribed distributions of atomization dispersity, mixture ratio, and flow intensity in the mixture-formation zone [1]. Liquid atomization is the process of disintegrating a bulk liquid into accumulated droplets. The disintegration process is initiated with the introduction of disturbances. The disturbances are in the form of either turbulence, inertial effects, or changes in velocity profile (flow relaxation or bursting effects) [2] which induce the formation of waves on the surface of liquid jets and sheets. If the conditions permit, the amplitudes of these waves may overgrow, resulting in instability and the further breakup of the liquid jets and sheets.

Numerous spray/atomization mechanism theories have been developed to describe the disintegration process. Pressure atomization is one group of atomization mechanisms. The main characteristic of this group of atomization is the ejection of fluids with high velocity through a small discharge orifice. The energy for atomization is the potential energy and is subsequently transferred into kinetic energy within the discharge orifice.

Plain orifice atomization is one example of pressure atomization with a simple orifice design to produce a liquid jet. This type of atomizer has been used in many applications, including industrial spraying, inkjet printers, and diesel and rocket engine propulsion devices due to its inherent simplicity and practicality [3]. Another example of pressure atomization is swirl atomization. Swirl atomization produces a spray by applying swirling effects on the liquid through tangential inlets or swirling inserts. The swirling motion pushes the flow close to the wall to create a low-pressure zone along the centerline, resulting in the air flowing back to the nozzle and forming an air-cored vortex. The convergent section near the discharge orifice accelerates the flow before exiting the atomizer [4].

Another group of atomization mechanisms is called pneumatic atomization. Pneumatic atomization is also known as twin-fluid atomization and is a type of liquid atomization that uses the movement of gas or vapour as the primary source of energy to produce spray [5]. Pneumatic atomization can be divided into (i) internal mixing and (ii) external mixing. Internal mixing has several advantages in practical applications, such as good atomization quality at low operating pressures, insensitivity to the changes of liquid viscosity, resistance to blockages of the discharge orifice, flexible control of spray characteristics, and low gas consumption rates compared to the external-mixing [6]. An example of internal mixing atomization is effervescent atomization. Effervescent atomization uses a small amount of air/gas injected into the mixing chamber and forms bulk liquid with dispersed bubbles. The bubbles expand as it discharges and shreds the bulk liquid into fine droplets [7].

Liquid disintegration regime maps graphically depict how a continuous liquid stream fragments into droplets as key parameters vary. By charting non-dimensional numbers (e.g., Reynolds, Weber, Ohnesorge), these maps delineate distinct breakup stages—from dripping and Rayleigh instability to wind-induced and full atomization—offering a clear visual framework for spray behaviour. Mapping an atomization regime is vital for atomizer design and process optimization. Such maps reveal the thresholds at which inertial, viscous, and aerodynamic forces dominate, enabling engineers to select operating conditions that yield desired droplet sizes, spray angles, and uniformity. Without regime maps, adapting atomization systems to application-specific requirements relies on costly trial and error. Theoretical studies of primary jet instability underpin these practical maps. Ibrahim [4] and Shinjo and Umemura [8] showed that analyzing the growth of surface perturbations and vortex dynamics in liquid jets not only elucidates core atomization mechanisms but also refines predictive models for droplet formation.

Research has been conducted for swirl effervescent atomization on various parameters (gas core [9], breakup length [10]–[12], spray angle [12]–[16], discharge coefficient [17], and Sauter mean diameter [18]) but a broader picture, such as the liquid disintegration regime is still barely available. Hence, studies are required to construct a liquid disintegration regime map for swirl effervescent atomization. The first stage of the study is to review the related liquid disintegration regime of swirl effervescent atomization, which are plain orifice atomization, swirl atomization, and effervescent atomization. This will assist the understanding of liquid disintegration in swirl effervescent atomization.

This article is organized as follows. Section 2 reviews the liquid disintegration regime of plain orifice atomization, which includes the jet stability curve and Ohnesorge plot. Section 3 comprises a review of the liquid disintegration regime of swirl atomization. Section 4 consists of a review of the liquid disintegration regime of effervescent atomization. Section 5 integrates this understanding and reports the hypothesis for the swirl effervescent disintegration regime. The conclusions of this review are reported in Section 6.

Nomenclature

a	liquid jet radius
D	droplet diameter
d_o	discharge orifice diameter
d_p	inlet port diameter
E_b	Bubble energy
g	Gravitational acceleration
L_{BU}	Jet breakup length
l_p	inlet port length
l_o	discharge orifice length
$\dot{m}_G$	Gas mass flowrate
$\dot{m}_L$	Liquid mass flowrate
Oh	Ohnesorge number
P_a	Air pressure
P_G	Gas pressure

Int. Journal of Integrated Engineering Vol. 17 No. 9 (2025) p. 85-116

P_L	Liquid pressure
R	Gas constant
Re	Reynolds number
Re_{crit}	Critical Reynolds number
T	Temperature
U_L	Jet velocity
We	Liquid Weber number
We_G	Gas Weber number
SMD	Sauter mean diameter
σ	Liquid surface tension
ρ_L	liquid density
μ_L	liquid viscosity
$\omega_{r,max}$	maximum pulsation
η_o	interface displacement
$\dot{x}$	quality or dryness

2. Liquid Disintegration Regime of Plain Orifice Atomization

The disintegration of liquid emanating from plain orifice atomizer is usually described using two methods: i. jet stability curve and ii. Ohnesorge plot.

2.1 Jet Stability Curve

Jet stability curve is a common way of describing the disintegration of cylindrical liquid jets. Jet stability curve is a plot of jet breakup length, L_{BU} versus jet velocity, U_L. Their relation can be expressed as:

$$L_{BU} = \frac{U_L}{\omega_{r,max}} ln\left(\frac{a}{\eta_o}\right) \quad (1)$$

where L_{BU} = jet breakup length (mm), U_L = jet velocity (mms^{-1}), $\omega_{r,max}$ = maximum pulsation (s^{-1}), a = liquid jet radius (mm) and, η_o = interface displacement (mm).

A typical liquid disintegration of cylindrical liquid jet described by Dumuochel et al. [19] involves five regimes which are (i) dripping regime, (ii) Rayleigh regime, (iii) first wind-induced, (iv) second wind-induced, and (v) atomization. Liu [2] categorizes "idealized" modes of liquid disintegration as (i) liquid dripping, (ii) liquid column/jet breakup, (iii) liquid ligament breakup, (iv) liquid sheet/film breakup, and (v) liquid free surface breakup.

The dripping regime can be described by the condition where droplets discharge the atomizer without the formation of a continuous liquid column [19]. The resultant droplets, also known as hanging/pendant droplets, form under the influence of gravity [2], [20], [21]. Theoretically, whenever the gravity force on the liquid is higher than the surface tension force, liquid will be pulled away. The formation of drops by a dripping mechanism inevitably entails large drops and low flow rates [22]. The droplet diameter can be determined as:

$$D = \left(\frac{6d_o\sigma}{\rho_L g}\right)^{1/3} \quad (2)$$

where D = droplet diameter (m), d_o = discharge orifice diameter (m), σ = liquid surface tension (kgs^{-2}), ρ_L = density (kgm^{-3}) and, g = gravitational acceleration (ms^{-2}).

An analysis conducted by Rayleigh for an inviscid jet in a vacuum revealed that all disturbances on a jet with wavelengths greater than its circumference will grow [23]. The Rayleigh mechanism of breakup shows the average drop size is nearly twice the diameter of the undisturbed jet or the discharge orifice diameter [22] and can be written as:

$$D = 1.89d_o \quad (3)$$

Weber extended the analysis of Rayleigh for viscous liquids and derived the relation of droplet diameter as [24]:

$$\frac{D}{d_o} = 1.436\left(1 + 3\frac{\mathrm{We}^{0.5}}{Re}\right)^{1/6} \tag{4}$$

Where We is the Weber number, and Re is the Reynolds number. The Weber number can be defined as in Eqn. (5), and the Reynolds number can be defined in Eqn. (6).

$$We = \frac{\rho_L U_L^2 d_o}{\sigma_L} \tag{5}$$

$$Re = \frac{\rho_L U_L d_o}{\mu_L} \tag{6}$$

The first wind-induced influence is the initiation of aerodynamic influence on the liquid. This is the regime where sinuous oscillations occur which result in droplet sizes comparable to the jet thickness [25]. This regime is characterised by the disintegration of a liquid jet subject to axisymmetric waves [24]. The increase in the jet velocity distorts the existing axisymmetric waves and forms asymmetric waves. Prior to the formation of the second wind-induced regime, air accelerates along the vicinity of convexities and decelerates along the vicinity of concavities. Hence, a low aerodynamic pressure develops in convexities, and high pressure develops in concavities of the liquid jet, which results in distortions of the initial wave from axisymmetric to asymmetric [24].

A fully developed spray characterised by spontaneous jet breakup into small droplets is known as an atomisation regime. This final regime can be described by rapid liquid disintegration with short or almost non-existent breakup length. Reitz [26] defined the atomisation regime as a complete jet disruption at the nozzle exit which produces average drop diameters much less than the jet diameter. The jet stability curve depicted by Lefebvre and McDonell [22] associated with typical flow regions, i.e., laminar, transition and turbulent flows, is shown in Fig. 1.

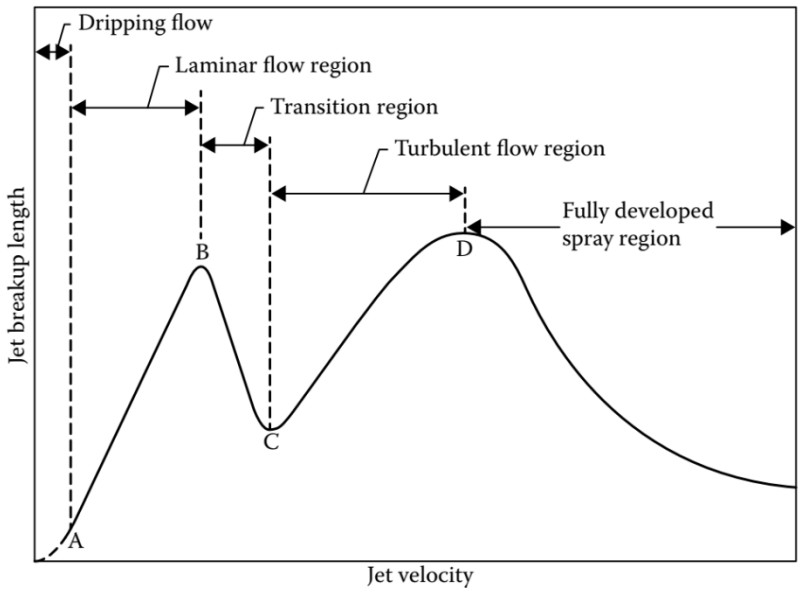

Fig. 1 *Jet stability curve associated with typical flow region. From [21]*

No et al. [27] and Lim et al. [28] analysed factors affecting the critical Reynolds number in the jet stability curve. The critical Reynolds number is the minimum Reynolds number at which breakup length is no longer increased with jet velocity but starts to decrease (point B in Fig. 1). No et al. [27] proposed an empirical correlation for sharp-edged, re-entrant, and convergent inlet atomisers. The empirical correlation is:

$$Re_{crit} = 218Oh^{-0.338}\left(\frac{l_p}{d_p}\right)^{0.086} \quad (7)$$

where Oh = Ohnesorge number, l_p = inlet port length and dp = discharge orifice length. It should be noted that the correlation is not valid for round-edged inlets.

Lim et al. [28] proposed new empirical correlations for two groups of inlet ports which are (i) (i) sharp-edged and re-entrant inlets and (ii) round-edged and convergent inlets. The proposed empirical correlation is due to the dependence of the critical Reynolds number on the discharge orifice length-to-diameter ratio. The empirical correlations obtained are:

For group 1 (sharp-edged and re-entrant inlet):

$$Re_{crit} = 175Oh^{-0.33}\left(\frac{l_p}{d_p}\right)^{0.15}\left(\frac{P_G}{P_a}\right)^{-0.18} \quad (8)$$

For group 2 (round-edged and convergent inlet):

$$Re_{crit} = 635Oh^{-0.39}\left(\frac{l_p}{d_p}\right)^{-0.28}\left(\frac{P_G}{P_a}\right)^{-0.19} \quad (9)$$

where Pg and Pa are gas pressure and air pressure, respectively.

Van de Sande and Smith [29] also proposed a correlation between the critical Reynolds number and the discharge orifice length-to-diameter ratio as:

$$Re_{crit} = 12000\left(\frac{l_o}{d_o}\right)^{-0.3} \quad (10)$$

The instability of the liquid jet associated with peculiarities observed in experimental work most probably arises from differences in the velocity profile and turbulence properties of the jet as it discharges from the nozzle. A numerical investigation conducted by Bravo et al. [30] revealed that transition to turbulence is significantly enhanced by the flow separation at the sharp corner of the nozzle inlet. Once the flow is transitioned to turbulence, the disintegration is quickly changed to turbulent atomisation, where the surface breakup occurs at the nozzle exit instead of axisymmetric instability wave developments. They also found that a more viscous liquid jet disintegrates more quickly and generates finer droplets with faster penetration speed. A similar phenomenon was observed by Khavkin [31] for swirl atomisers, and he stated that viscosity helps droplets to stretch. However, Khodayari [32] contrastingly observed that viscosity dampens the growth rates of instability and leads to a longer breakup length.

Sallam et al. [33] studied the new measurement of breakup length for turbulent liquid jets in quiescent air with greater emphasis on conditions where small Reynolds numbers and aerodynamic effects were anticipated. They summarised available data from literature and gave the following correlation of the breakup length for common fluids, such as water and ethanol:

$$\frac{L_{BU}}{d_o} = 5We^{0.5} \quad \text{; for We < 400} \quad (11)$$

The correlation by Sallam et al. [33] in Eqn. 11 was numerically tested by Pan and Suga [34] for the accuracy with the We-L_b/d_o plot shown in Fig. 2. They set the mean values in Fig. 2 by averaging the instantaneous breakup length over a period of time during which the jets go through the distance of five times as long as the computational domain in the axis direction. They observed a reasonably good agreement for all the cases presented.

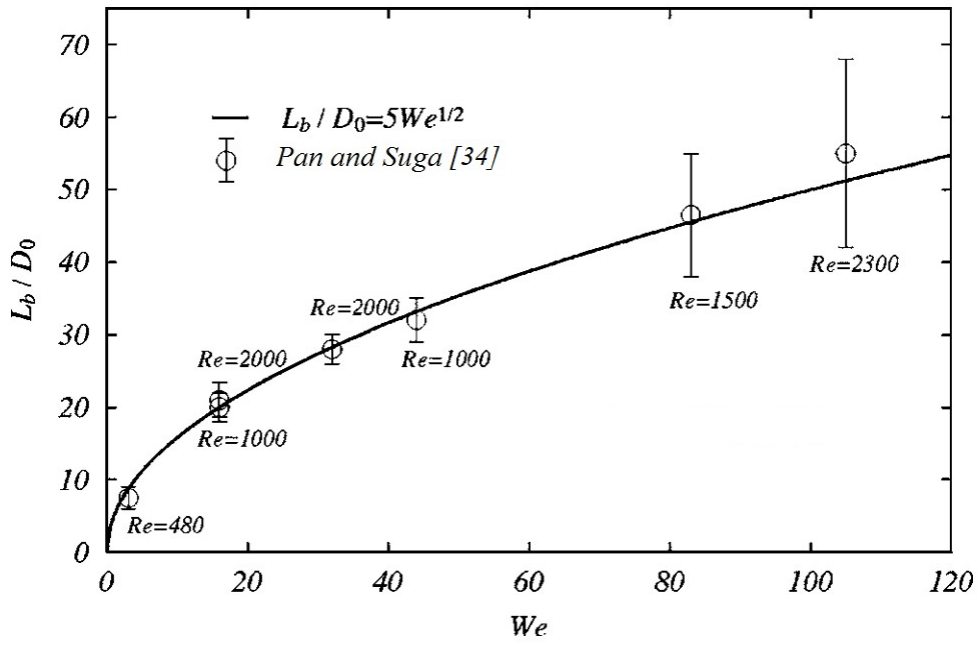

Fig. 2 *Comparison of breakup length of laminar jets at different Weber numbers. From [34]*

Etzold et al. [35] constructed a jet stability curve for their fabricated nozzle and compared their experimental results with the theory proposed by Sterling and Sleicher [36]. They found that their experimental results did not agree with results derived from existing models or with experimental data from literature. They attributed the cause of the discrepancies to the properties of the gas boundary layers around the liquid jets. At relatively small ambient Reynolds numbers, the ambient influences decrease, which causes an increase in jet length. Etzold [35] proposed a modification to the Sterling and Sleicher [36] theory and observed good agreement of the modified theory with their experimental data. The plot of the modified model and the experiment of Sterling and Sleicher [36] is shown in Fig. 3.

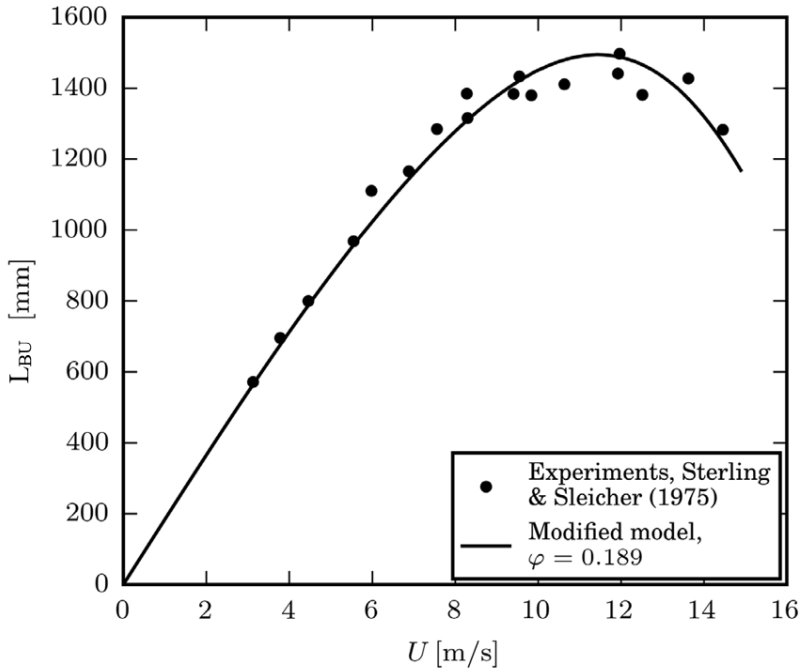

Fig. 3 *Plot by Etzold et al. [35] to fit their proposed modified model with the experimental works of Sterling and Sleicher [36]*

Int. Journal of Integrated Engineering Vol. 17 No. 9 (2025) p. 85-116

Arai et al. [37] investigated plain orifice atomisers in diesel spray applications. They varied the ambient pressure to simulate elevated pressure and temperature in a diesel combustion chamber. They found that ambient pressure influence on the jet breakup length is enormous and essential. An increase of ambient pressure from 0.1 MPa to 3.0 MPa resulted in a significant shortening of the jet breakup length.The jet stability curve flattens with the increase in ambient pressure. The effect of ambient pressure on the spray breakup length was also reported by He et al. [38], Fu and Yang [39], and Leroux et al. [40]. Leroux et al. [40] observed three conditions of a liquid jet disintegration subjected to three ambient pressures. In a state in which the value of the ambient pressure is lower than the atmospheric pressure (1 atm), the physical characteristics of the liquid jet become the significant factor for jet disintegration without the influence of the surrounding gas. However, this phenomenon differs when the ambient pressure is less than 1 atm, where the effect of aerodynamic forces becomes dominant. The third situation is when the ambient pressure is approximately equal to 1 atm. Both the effect of jet physical characteristics and aerodynamic forces take place in disintegrating the liquid jet.

Yang et al. [41] found that the effect of gas density is more dominant in the atomisation of a viscoelastic jet. This was also discovered by Zhang and Shin [42] and Spangler et al. [43] for general jets. Spangler et al. [43] portrayed the findings in a plot of gas Weber number versus jet breakup length as shown in Fig. 4. The plot shows the variation of the jet stability curve with density ratio, ϵ, which is defined as:

$$\epsilon = \frac{\rho_L}{\rho_G} \tag{12}$$

Where ρ_L and ρ_G are liquid and gas density, respectively.

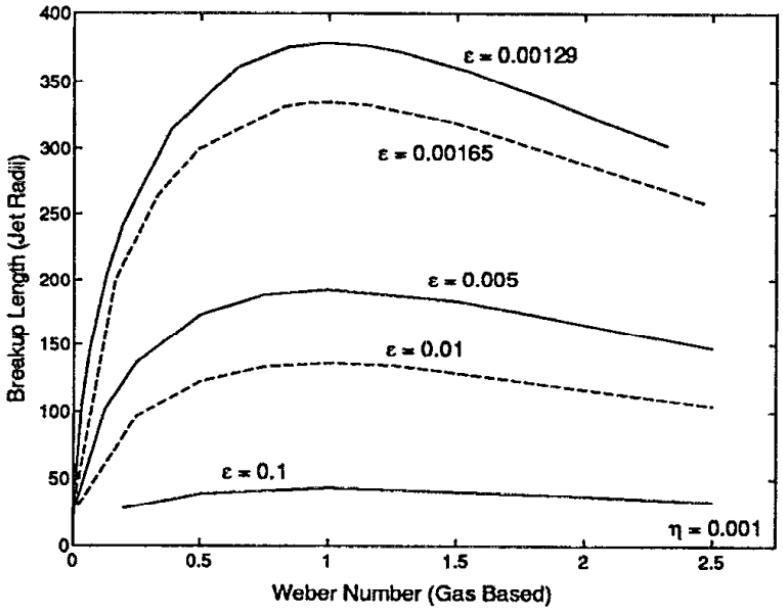

Fig. 4 *Jet stability curve proposed by Spangler et al. [43]*

2.2 Ohnesorge Plot

Ohnesorge [44] illustrated liquid disintegration regimes for plain orifice atomisation into three sections. These sections depend on the liquid Reynolds number and a dimensionless number that contains only liquid properties (Ohnesorge number, Oh). The Ohnesorge's liquid disintegration regime map for plain orifice atomisation is plotted as an Re-Oh plot, which is described below and shown in Fig. 5.

- At low Reynolds numbers, disintegration of the liquid jet into large drops of uniform size occurred and was named the Rayleigh mechanism of breakup.
- At intermediate Reynolds numbers, jet oscillations with respect to the jet axis are the source of the jet breakup. The magnitude of these oscillations increases with air resistance until the liquid jet completely disintegrates. A wide range of drop sizes is produced.
- At high Reynolds numbers, atomisation is complete within a short distance from the discharge orifice.

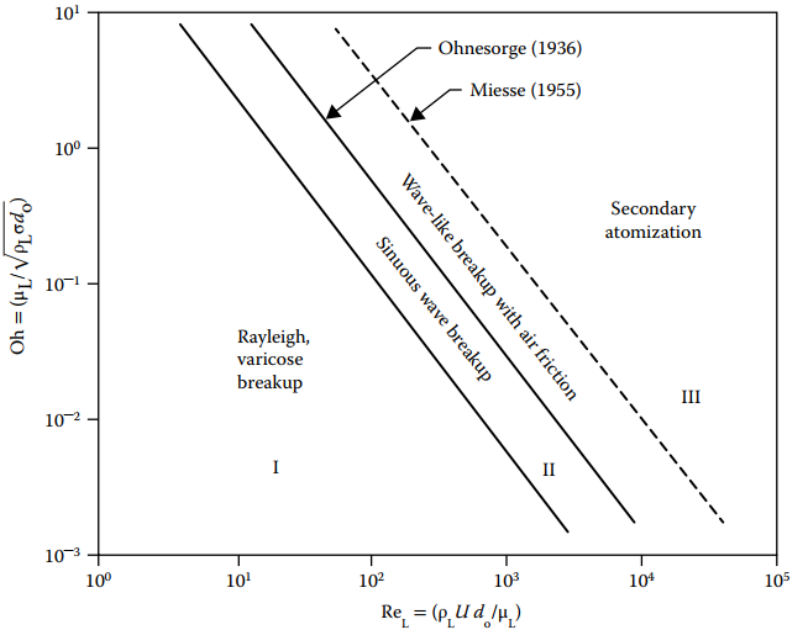

Fig. 5 *Regimes of liquid disintegration in plain orifice atomization by Ohnesorge [44]*

Ohnesorge number, Oh can be written as:

$$Oh = \frac{\sqrt{We}}{Re} \tag{13}$$

These liquid disintegration regimes proposed by Ohnesorge [44] have been corrected by Reitz [26] into four regimes, which include (i) the (i) Rayleigh mechanism, (ii) first wind induced, (iii) second wind induced, and (iv) atomisation. The liquid disintegration regimes map is shown in Fig. 6 with detailed descriptions of the map.

Considering the Ohnesorge number between 0.001 and 0.01, the mechanism of liquid disintegration of Fig. 6 can be described as follows:

- At Reynolds numbers 10 to 100, the surface tension induces the disintegration of a liquid jet (*Rayleigh regime {1})* symmetric, or varicose instability) into nearly identical droplet sizes.
- At Reynolds numbers 1000 to 10000, aerodynamic forces influence the formation of drops (nonaxisymmetric Rayleigh breakup). These forces cause symmetric (*first wind-induced regime* {2}) and asymmetric (*second wind-induced regime* {3}, asymmetric or sinusoidal instability) wave growth of the gas–liquid interface that finally leads to jet disintegration. This is called an aerodynamic regime.
- At a Reynolds number approaching 100000, the jet disintegrates almost immediately at the discharge orifice. This mode is called the *atomisation regime* {4}. The spontaneous disintegration could be explained with this statement: Ohnesorge number is a dimensionless number that contains only liquid properties (viscosity and surface tension) or, mathematically, $Oh = \frac{\mu}{\sigma}$. A small Ohnesorge number represents either a decrease in viscosity or an increase in surface tension. According to Hilbing and Heister [45], an increase in surface tension led to a rapid growth of the wave formed on the surface of the jet from the unsteady inflow, which led to shorter breakup.

Int. Journal of Integrated Engineering Vol. 17 No. 9 (2025) p. 85-116

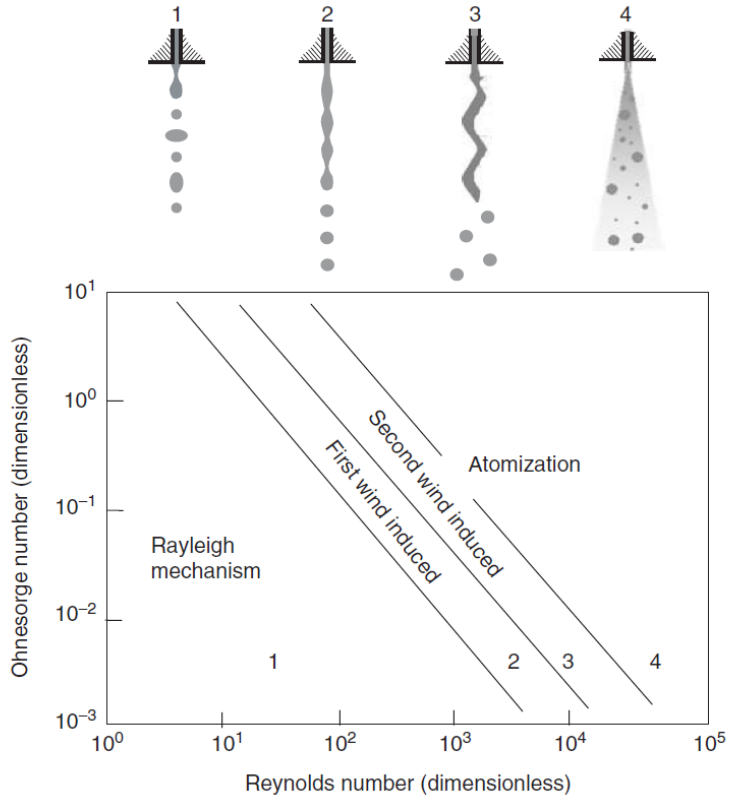

Fig. 6 *Regimes of liquid disintegration in plain orifice atomization by Reitz [26]*

Wang and Fang [46] examined the effect of discharge orifice shape variation on the liquid disintegration of plain orifice atomisation. They observed shifting of the boundary in the regimes of liquid disintegration by Ohnesorge [44], as shown in Fig. 7. It is shown in Fig. 7 that liquid jets discharging from triangular and square-shaped orifices move the boundary lines dividing different regimes to the left (lower Reynolds number). They also noticed the transition bridging the Rayleigh breakup regime and the wind effects-dominant regime is narrowed to some extent. A more interesting finding is that the wind-induced effect is introduced into the breakup process much faster for the triangular jets than for the other three shapes (circular, rectangular, and square).

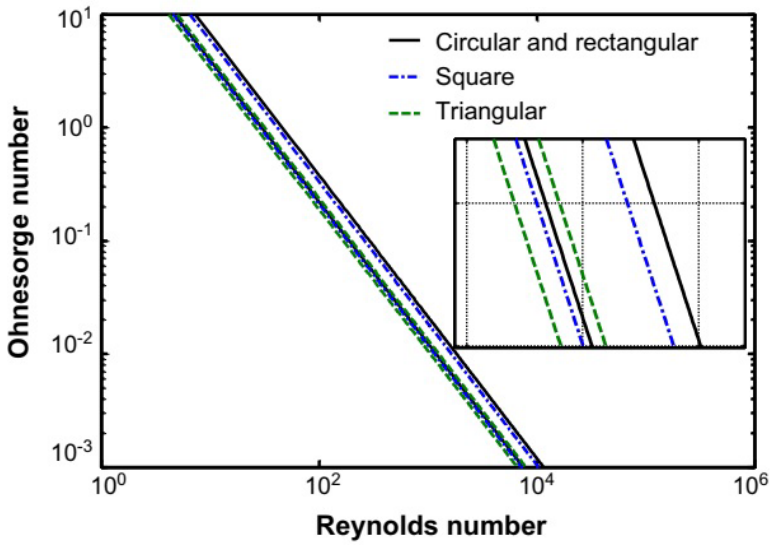

Fig. 7 *Modified Ohnesorge [44] plain orifice liquid disintegration regime by Wang and Fang* [46] *for non-circular orifice*

2.3 Summary on plain orifice atomization

Generally, the plain orifice atomisation regime transitions from low-energy dripping to high-energy full atomisation as inertial and aerodynamic forces begin to dominate over surface tension. Initial breakup occurs through Rayleigh instability, leading to wind-induced disintegration and, eventually, chaotic turbulent atomisation.

Modifications were made to the original jet stability curve, or Ohnesorge plot, for further understanding of the plain orifice atomisation. Sallam et al. [33] and Pan and Suga [34] replotted the jet stability curve of U_L vs L_{BU} into We vs L_{BU}/d_o. Arai et al. [37] studied the jet stability curve at different ambient pressures. Spangler et al. [43] observed variation of the jet stability curve with the gas-liquid density ratio. Leorux et al. [40] observed 3 ambient pressure effects that could distinguish the jet stability curve into 3 types. Wang and Fang [46] portrayed the effect of a non-circular orifice on the transition between regimes.

3. Liquid Disintegration Regime of Swirl Atomization

Liquid disintegration of swirl atomisation as classified by Lefebvre and McDonell [22] involves five stages of development as shown in Fig. 8. The stages can be described as follows:

- Dribble stage: liquid dribbles from the orifice.
- Distorted pencil: liquid leaves as a thin distorted pencil.
- Onion stage: a cone forms at the orifice but is contracted by surface tension forces into a closed bubble.
- Tulip stage: the bubble opens into a hollow tulip shape terminating in a ragged edge, where the liquid disintegrates into large drops.
- Fully developed spray: the curved surface straightens to form a conical sheet. As the sheet expands, its thickness diminishes, and it soon becomes unstable and disintegrates into ligaments and then drops in the form of a well-defined hollow-cone spray.

The disintegration of liquid in swirl atomisation initially involves disintegration of the cylindrical liquid jet depicted by the dribble and 'distorted pencil' stages before the disintegration of the liquid sheet with expansion of the spray angle, which results in the initiation of the onion stage and ends with a fully developed spray.

Fung et al. [47] conducted an analysis on the liquid disintegration by a nasal spray device. They experimentally observed that for a low-pressure spray (under 5 bar compression pressure), the spray development is in agreement with Lefebvre and McDonell [22], as shown in Fig. 9. Another example of spray structures discharged from a swirl atomiser, which has good agreement with Lefebvre and McDonell [22], was illustrated by Dafsari et al. [48], as shown in Fig. 10.

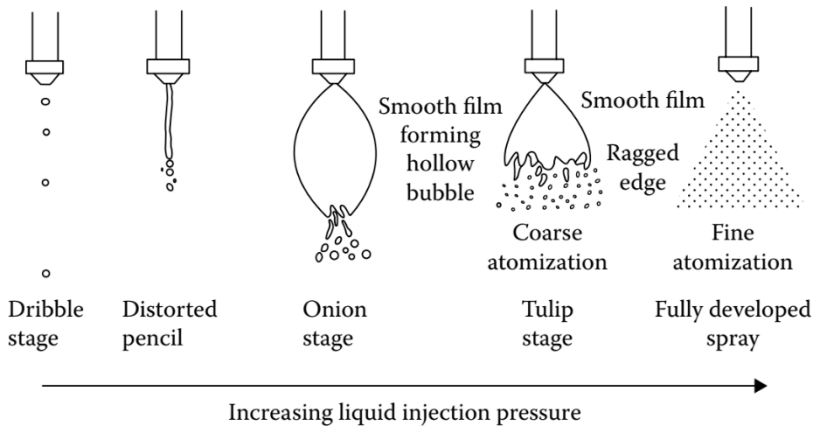

Fig. 8 *Stages of liquid disintegration in swirl atomisation. From Lefebvre and McDonell [22]*

Int. Journal of Integrated Engineering Vol. 17 No. 9 (2025) p. 85-116

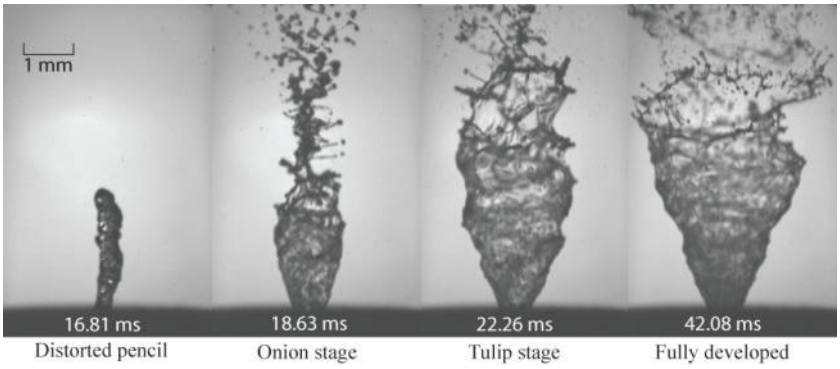

Fig. 9 *Stages of liquid disintegration of a nasal spray device under 5 bar compression pressure. From Fung et al.* [47]

Laurila et al. [49] studied a large-scale pressure-swirl atomiser using large-eddy simulation. They focused on liquid atomization of a highly viscous liquid. Their simulations did not illustrate onion and tulip shapes as the near field spray patterns, but they observed an S-shaped liquid film spray formed at Re = 420. They concluded that the results may be caused by the nonuniform velocity distribution at the discharge orifice. Yao [21] has also conducted an analysis of highly viscous fluids emanating from swirl atomizers. They observed that the stages of liquid disintegration retracted back to earlier stage with the increase of viscosity (onion stage turns into distorted pencil). Similar observations were acquired by Park et al. [50]. This may be attributed to suppression in the increase of maximum disturbance growth rates by liquid viscosity as observed by Yan et al. [51]. Yao [52] also found that although an increase in viscosity produces similar spray patterns at early discharge (~290ms), further temporal evolution depicts otherwise as shown in Fig. 11.

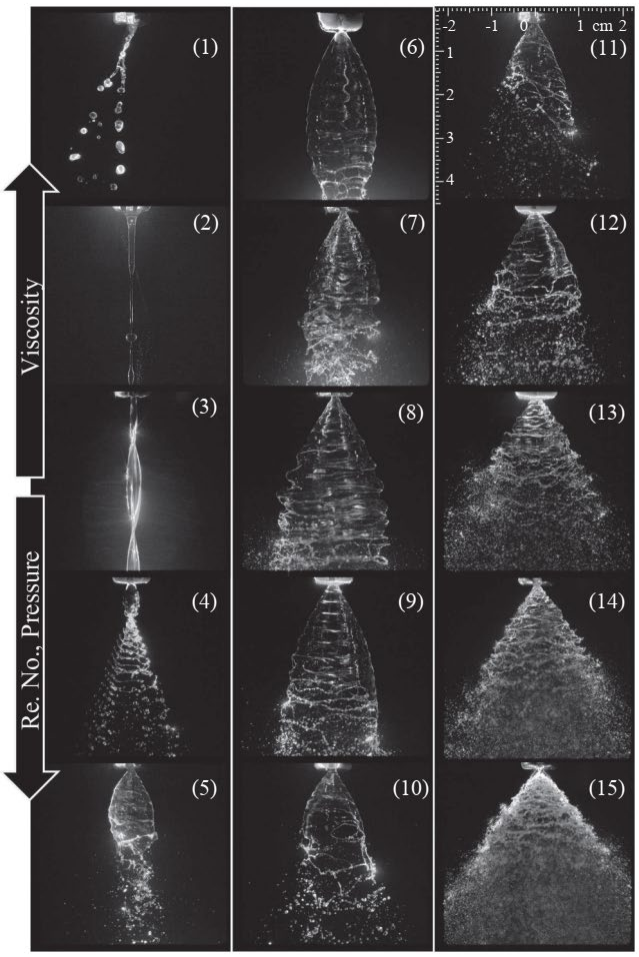

Fig. 10 *Stages of liquid disintegration of swirl atomizer emanates alternative aviation fuel by Dafsari et al. [48]. *Image 1: high viscosity, low Re; Image 15: low viscosity, high Re.*

Rhim and No [53] performed atomization of neat light oil and emulsified fuels via a swirl atomizer. They observed that the liquid disintegration of both liquids follows the stages of liquid disintegration in swirl atomization illustrated by Lefebvre and McDonell [22]. Specifically, the onion stage occurs below 0.2 MPa for neat light oil and emulsified fuel with the water content of 20%. The tulip stage occurs between 0.2 and 0.4 MPa for neat light oil, between 0.2 and 0.6 MPa for the emulsified fuel with the water content of 20%, and between 0.1 and 0.8 MPa for the emulsified fuel with the water content of 40%, respectively. Rhim and No [53] also constructed a liquid disintegration regime map of swirl atomization as shown in Fig. 12.

Kang et al. [54] conducted a review of swirl atomization in liquid rocket engine applications. They summarized the liquid disintegration of swirl atomization from the previous literature into seven stages include (i) dribbling, (ii) distorted pencil, (iii) onion shape, (iv) tulip shape, (v) wavy cone shape, (vi) perforated cone, and (vii) fully developed spray. They also found that if the liquid is in the form of a gel, the stages become (i) swirling jet, (ii) twisted ribbon, (iii) fluid web, and (iv) fully developed spray.

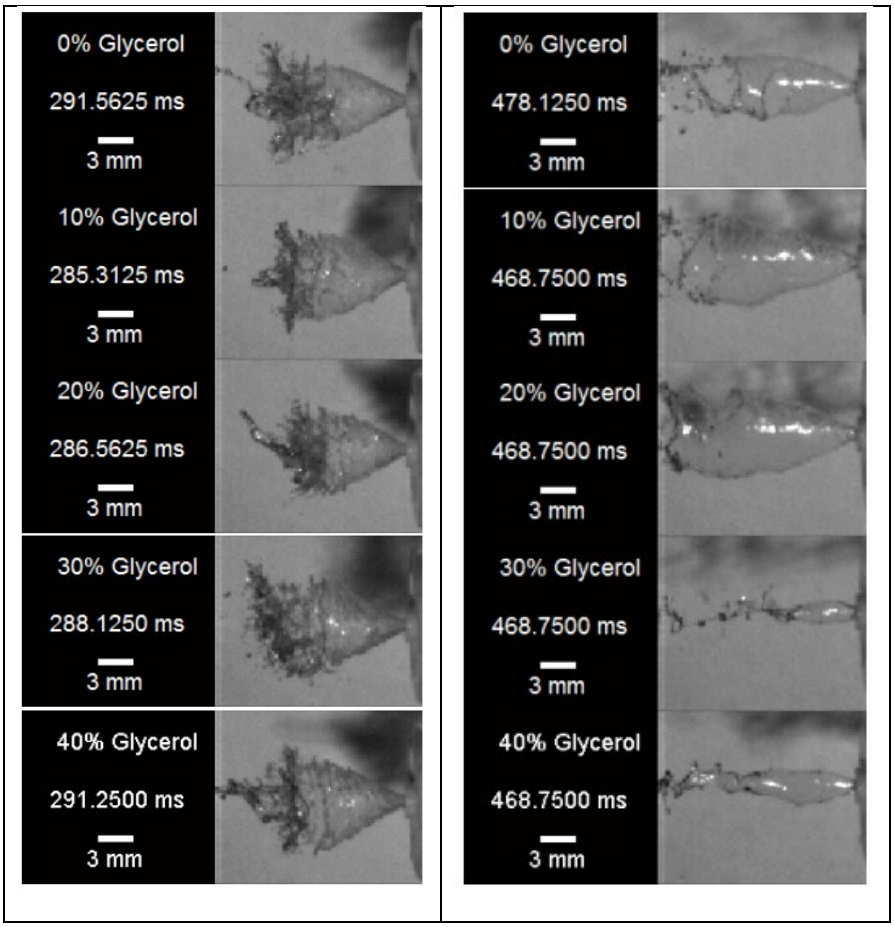

Fig. 11 *Temporal evolution of sprays from (a) ~290ms; to (b) ~470ms with different liquid viscosity. From [52]*

Int. Journal of Integrated Engineering Vol. 17 No. 9 (2025) p. 85-116

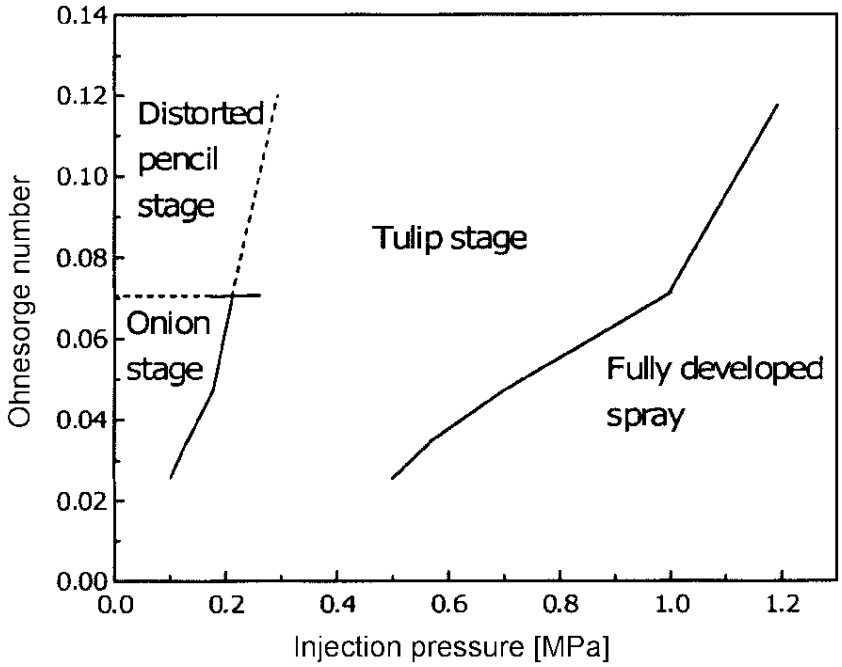

Fig. 12 *Liquid disintegration regime map of swirl atomization. From Rhim and No [53]*

Prakash et al. [55] related the stages of swirl spray disintegration to the Weber number. They observed that the dribbling stage remains until We = 161. At this value, the jet was observed to exhibit distorted pencil stage (Fig. 13a). A further increase in liquid Weber number (We = 250) turned the swirl jet to the onion stage (Fig. 13b). The significance of the swirling effect is observed with the initiation of a hollow cone prior to discharging the orifice. The inertial forces of the swirling liquid sheet are insufficient to overcome the surface tension forces. The disintegration of the expanding hollow cone is observed further downstream. The swirl jet exhibits the tulip stage at higher magnitudes of liquid Weber number (We = 664), as shown in Fig. 13c. The inertial force overcomes the surface tension to the extent that the hollow cone of the liquid sheet disintegrates before it is pulled back inwards, with growing waves formed on the sheet promoting the breakup. Fig. 13d shows the fully developed spray stage, which is generally observed at very high liquid Weber numbers where the dominant inertial forces are more significant compared to the surface tension forces. The hollow cone is fully developed, and aerodynamic forces dictate the breakup processes.

Ghorbanian et al. [56] observed a new stage between the tulip and fully developed stage known as the wavy mode at P = 0.5 bar. The annular waves have a longitudinal direction with respect to the atomizer axes and are the major cause of the sheet disintegration. They also observed that by increasing the injection pressure, the wave frequency increases, short-length waves develop, and the breakup length decreases. Ramamurthi and Tharakan [57] figured out the swirl spray change from the tulip stage to fully developed spray is in the range of $140<We<170$. They plotted the disintegration regime of the tulip stage (tulip-shaped) and fully developed spray (cone-shaped) on a Re-We map, as shown in Fig. 14.

The perforated stage for a swirl atomizer discharging a mixture of water and a polymer charge (a slightly non-Newtonian liquid) was observed by Sindayihebura and Dumouchel [58], as shown in Fig. 15. The perforated stage of a swirl atomizer was also observed by Loustalan et al. [59] and Najafi et al. [60].

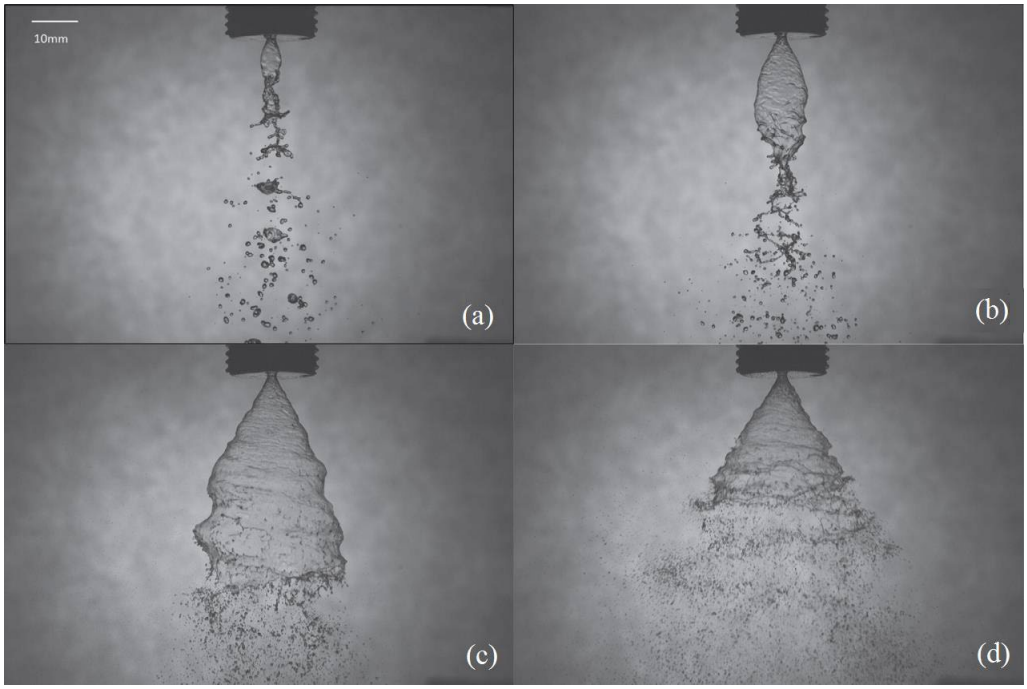

Fig. 13 *Disintegration stages of swirl spray with (a) We=161; (b) 250; (c) 664; and (d) >$664. From Prakash et al. [55]*

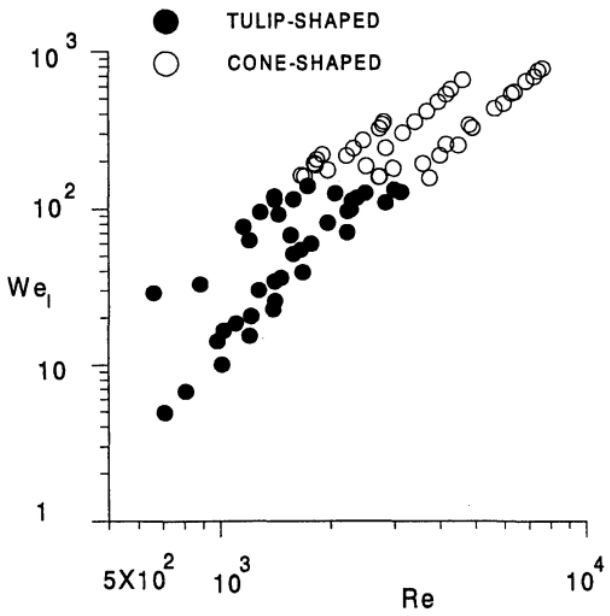

Fig. 14 *Liquid disintegration regime map of tulip and fully developed spray (cone-shaped) by Ramamurthi and Tharakan [57]*

Int. Journal of Integrated Engineering Vol. 17 No. 9 (2025) p. 85-116

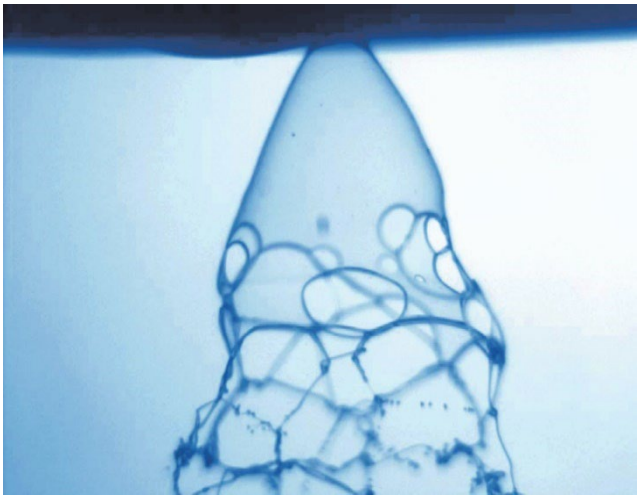

Fig. 15 *Perforated stage of conical liquid sheet. From Sindayihebura and Dumouchel [58]*

The results from the experimental investigation of Wang and Lefebvre [61], Jasuja [62], and Rashad et al. [63] were replotted in Fig. 16, Fig. 17, and Fig. 18, respectively, to illustrate part of the liquid disintegration regime of swirl atomization. Fig. 16 and Fig. 17 show that the influence of both the Ohnesorge number and Reynolds number on SMD are equally significant. At Ohnesorge number = 0.0055, SMD decreased with the increase of Reynolds number from 12500 to 3000 and reached the smallest SMD as it approaches Reynolds number = 30000. At Reynolds number = 12500, SMD spanned from the largest to the smallest with the increase of Ohnesorge number from 0.0055 to 0.0075. Fig. 18 shows that the largest SMD is found at Ohnesorge number > 0.0055 and Reynolds number < 20000. The smallest SMD is observed at 0.004 < Ohnesorge number < 0.0045 and 30000 < Reynolds number < 40000.

Fig. 16 to Fig. 18 show that the disintegration regimes of swirl atomization follows the disintegration regime trends of plain orifice atomization. The contour plots closely resemble the Ohnesorge plot for plain orifice atomization. Considering the displayed contour plot as fully developed sprays regime (SMD < 200 microns), the distribution of SMD may be used to predict other disintegration regimes.

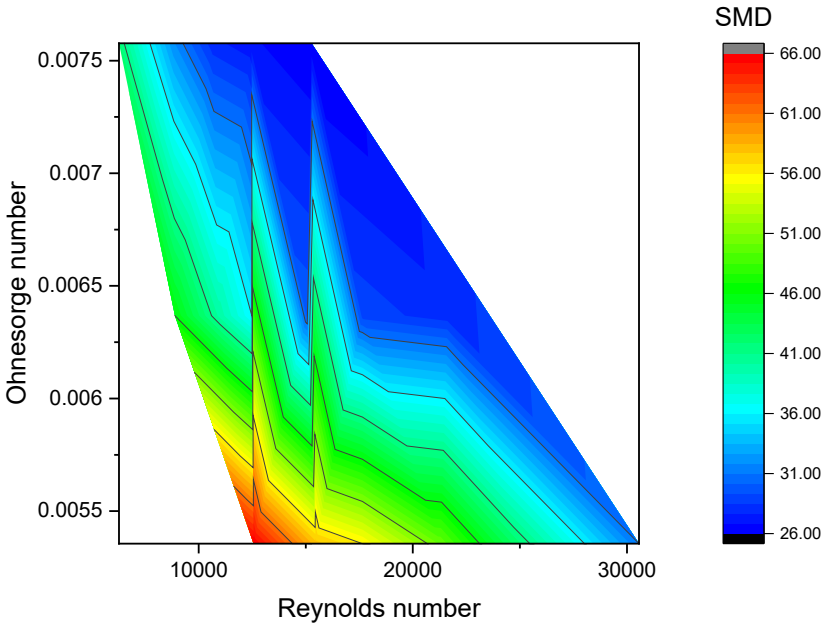

Fig. 16 *Replot experimental results of Wang and Lefebvre [61] as illustration to part of liquid disintegration regime map for swirl atomization*

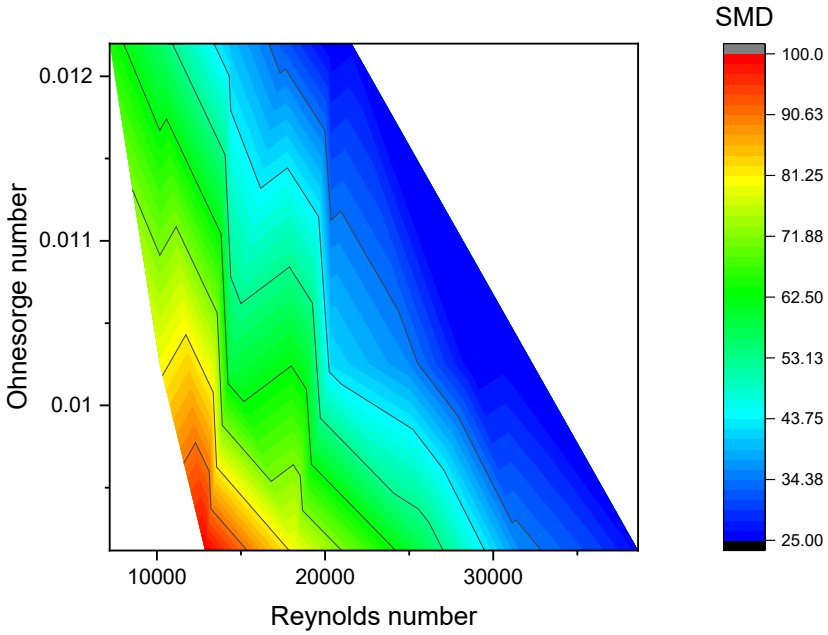

Fig. 17 *Replot experimental results of Jasuja [62] as illustration to part of liquid disintegration regime map for swirl atomization*

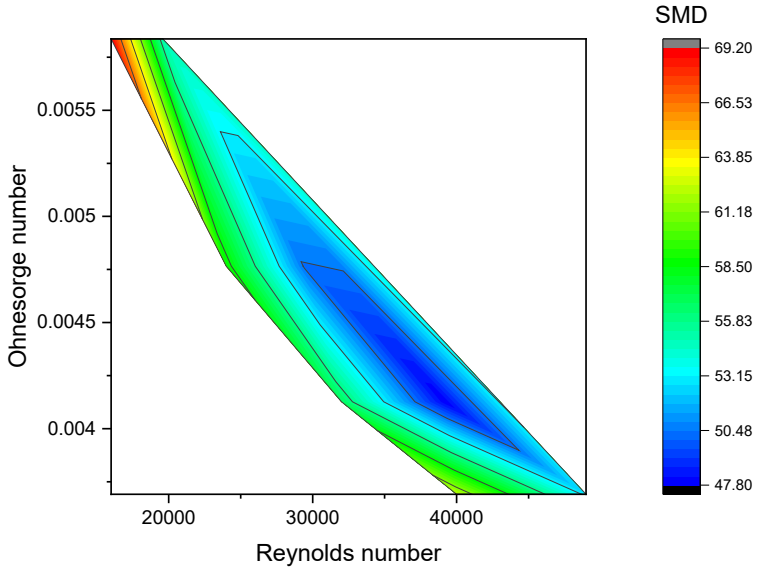

Fig. 18 *Replot experimental results of Rashad et al. [63] as illustration to part of liquid disintegration regime map for swirl atomization*

The liquid disintegration regimes for the swirl atomizer have also been extended to the spray cone angle. Vijay et al. [64] summarized the regimes of spray cone angle in swirl atomization into two groups based on three references (Group 1: Halder et al. [65] and Lee et al. [66] and Group 2: Kim et al. [67]. Table 1 below describes the spray cone angle regimes of the swirl atomizer.

Int. Journal of Integrated Engineering Vol. 17 No. 9 (2025) p. 85-116

Table 1 *Regimes of spray cone angle (Extracted from Vijay et al.* [64]*)*

Reference	Regimes of spray cone angle		Characteristics
Halder et al. [65],	1	Narrow cone angle	No air core
Lee et al. [66]	2	Marginal rise cone angle	Appearance of air core
	3	Constant cone angle	Air core extension (or development) up to swirl chamber
	4	Step rise in cone angle	Highly unstable air core
	5	Cone angle critical limit	Completely developed air core
Kim et al. [67]	1	Cone angle before breakup	With reference to the orifice exit and breakup point
	2	Cone angle after breakup	With respect to the breakup spot and the spatial size of droplet distribution

3.1 Summary on Swirl Atomization

Disintegration regimes of swirl atomization as observed by many researchers involve the dribble stage, distorted pencil, onion stage, tulip stage, and fully developed spray. However, viscosity may alter or impede the development of a regime. Analysis was conducted on a few researches by replotting their available data into a contour plot that represents the Ohnesorge plot. It was found that the trend resembles plain orifice atomization regimes. The distribution of SMD may be used to predict other disintegration regimes. Spray cone angle regimes also exist as reviewed by Vijay et al. [64].

4. Liquid Disintegration Regime of Effervescent Atomization

Effervescent atomization is a type of atomization which uses gas bubbles as the source for liquid disintegration. The mechanism of liquid disintegration in effervescent atomization was initiated with the discharge of air/gas bubble which explodes and shatters the liquid film into small droplets [68]–[70]. Gadgil and Raghunandan [71] observed three stages of disintegration of effervescent atomization namely (i) bubble formation and transport, (ii) bubble trapped inside a liquid jet, and (iii) bursting of bubble as shown in Fig. 19. The term "bursting of bubble" or "bubble bursting" referring to the explosion of bubble as the bubble exit the atomizer through the orifice. As the ambient pressure drops to atmospheric pressure, the energy carries by the bubble pushes the liquid film and initiates the bubble explosion or bursting.

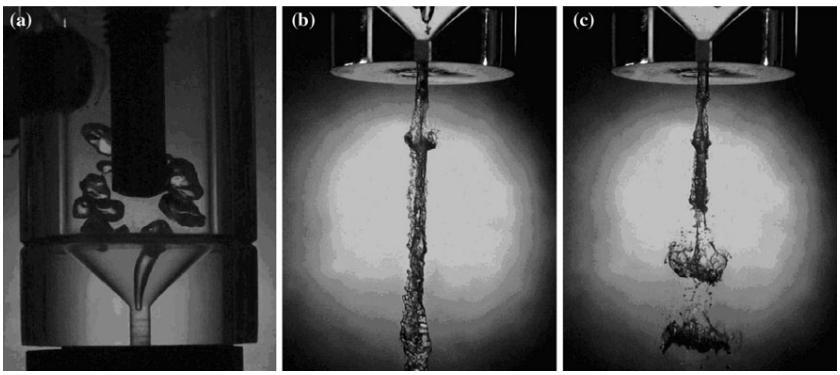

Fig. 19 *Disintegration in effervescent atomization. (a) bubble formation and transport; (b) bubble trapped inside a liquid jet; and (c) bursting of bubble. From Gadgil and Raghunandan [71]*

Santangelo and Sojka [72] denoted that the spray structures of effervescent atomization consisted of two regimes: (i) the bubbly flow regime and (ii) the tree regime. The regimes change with gas-to-liquid ratio (GLR). GLR was reviewed by Ghaffar et al. [73], [74], as the dominant independent parameters for effervescent atomizer. Chen et al. [75] observed that GLR not only affecting the droplet mean diameter but also the droplet proportion

within similar mean diameter. Sovani et al. [7] explained that the bubbly flow regime occurs with a GLR less than 0.02. Each gas bubble flowed consecutively through the discharge orifice and was surrounded by a liquid sheath. A liquid slug succeeded each bubble. After discharging from the orifice, the gas bubbles expanded rapidly, exploded, and shattered both the surrounding liquid sheath and, to some extent, the liquid slug into fine shreds. An illustration of this bubbly flow breakup mechanism is presented in Fig. 20. At GLRs greater than 0.05, the internal flow changed to the annular-flow regime. The central gas core, created by the coalescence of individual gas bubbles, expanded rapidly and broke up the annular sheath into a ring of ligaments. The near-nozzle structure in this regime resembled a tree with the annular liquid sheath forming a hollow trunk and the ligaments forming branches, as shown in Fig. 21.

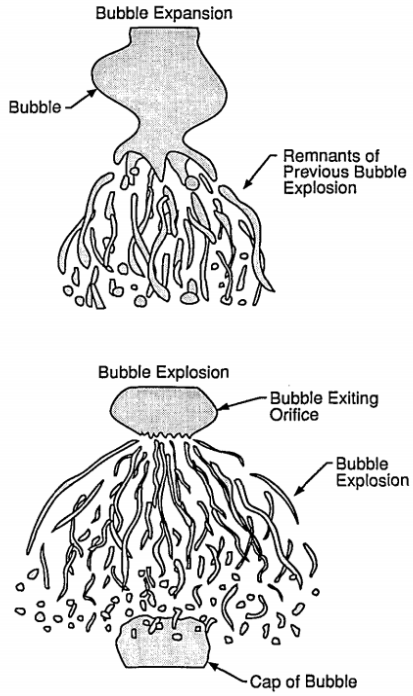

Fig. 20 *Bubbly flow regime near orifice of effervescent atomization. From Santangelo and Sojka [72]*

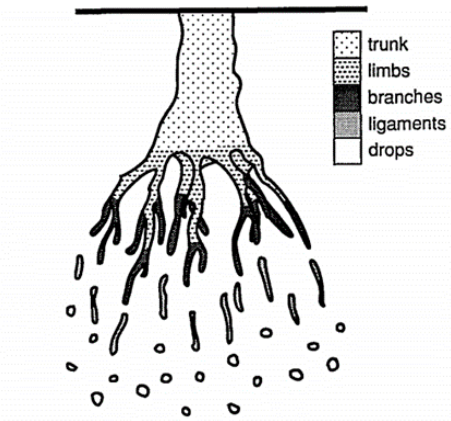

Fig. 21 *Tree regime near orifice spray structure. From Santangelo and Sojka [72]*

Zaremba et al. [76] analyzed effervescent atomization with different fluid injection configurations, which are: (i) outside-in-gas (OIG) and (ii) outside-in-liquid (OIL). Mlkvik et al. [77] described an OIG atomizer as an atomizer in which the creation of a two-phase flow is induced by the introduction of gas to the mixing chamber via a perforated aerator. The internal two-phase flow pattern for this type of atomizer is mainly affected by the pressure drop and the liquid and gas flow rates. The OIL atomizer uses a similar geometrical design to the OIG atomizer, but the inlet ports are switched. The air is introduced directly in the mixing chamber from the top, while the liquid

Int. Journal of Integrated Engineering Vol. 17 No. 9 (2025) p. 85-116

enters the atomizer through the perforated wall of the mixing chamber (the aerator in the OIG atomizer). The main difference between these configurations is the mixing mechanism of the flow components, as shown in Fig. 22. Zaremba et al. [76] denoted that liquid disintegration in effervescent atomizer with OIG configuration experiences four spray conditions as seen in Fig. 23. Zaremba et al. [76] also portrayed differences of resultant sprays by OIG and OIL as shown in Fig. 24.

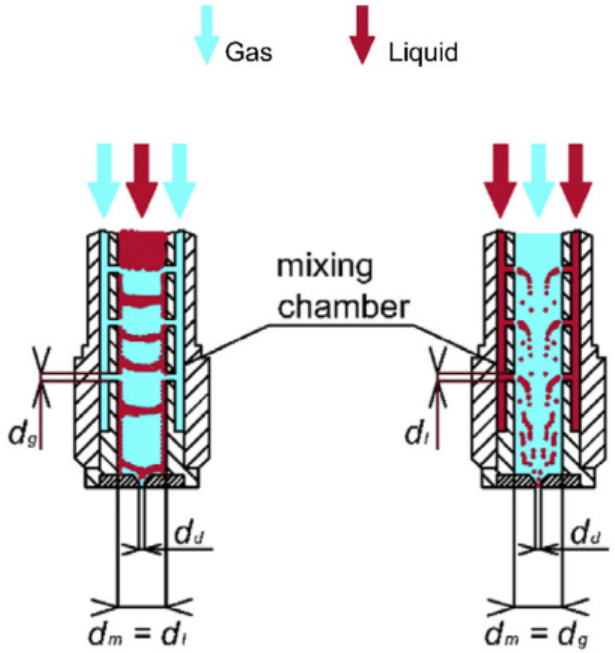

Fig. 22 *Schematic of (a) OIG; and (b) OIL atomizer. From Mlkvik et al. [77]*

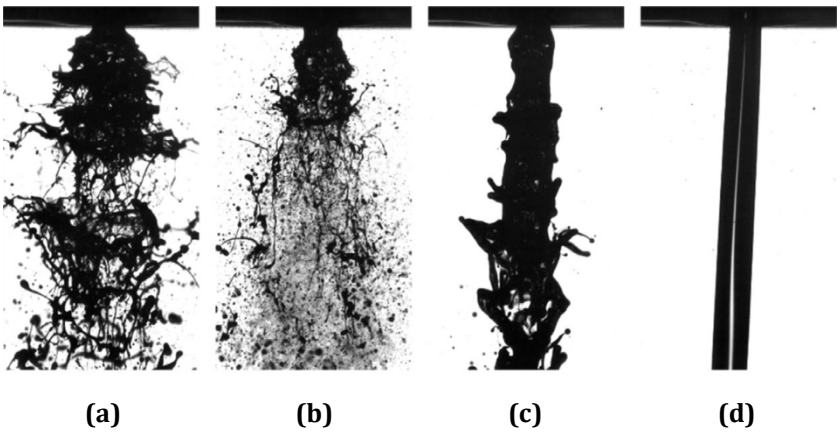

Fig. 23 *Disintegration of effervescent atomizer with OIG configuration: (a) explosions of bubbles; (b) explosions of large bubbles; (c) partial disruption of the liquid stream; (d) no disruption of the liquid stream. From Zaremba et al. [76]*

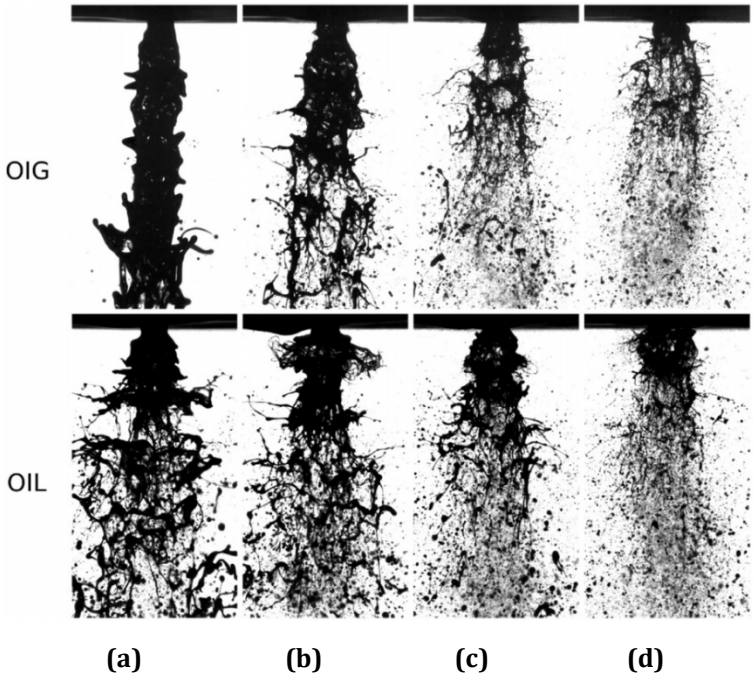

Fig. 24 *Comparison of OIG and OIL sprays with the changes of GLR: (a) 0.025; (b) 0.05; (c) 0.1; and (d) 0.2. From Zaremba et al. [76]*

Zaremba et al. [78] illustrated liquid disintegration of effervescent spray into seven stages including: 1) Bubble discharge, 2) Expansion of bubble, 3) The radial expansion is nearly finished, 4) Initiation of the liquid breakup, 5) Radial deformation of the liquid due to the gas expansion is finished and the axial acceleration enhances the breakup in the core of the spray, 6) Formation of large droplets and ligaments, created by the first gas bubble expansion, are now accelerated by the following expanding gas bubble, and 7) Ligaments are elongated, accelerated, and consequently disrupted by the combination of the acceleration of the expanding gas and by the interaction with the ambient atmosphere. The illustration is shown in Fig. 25.

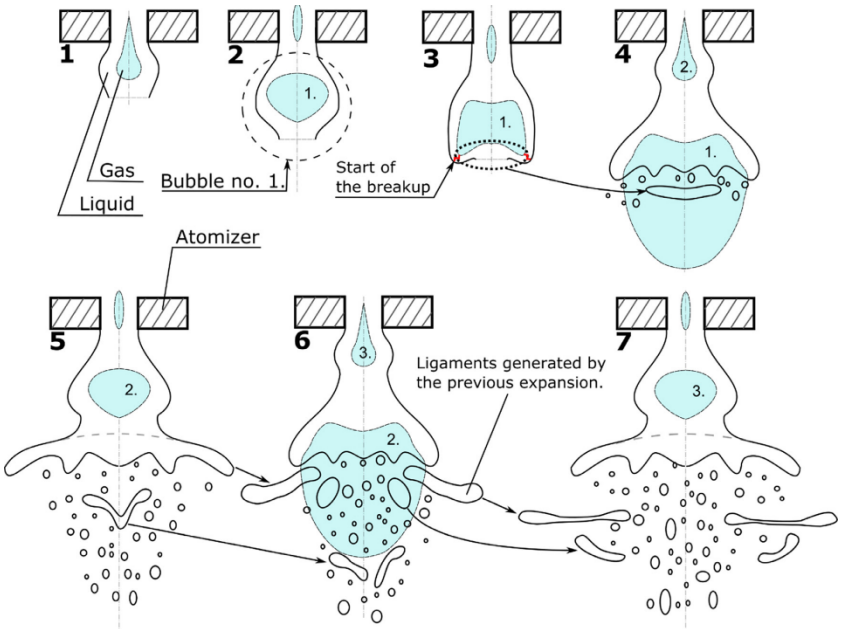

Fig. 25 *Illustration of disintegration stages of effervescent atomization. From Zaremba et al. [78]*

Int. Journal of Integrated Engineering Vol. 17 No. 9 (2025) p. 85-116

Broniarz-Press et al. [79] conducted a study on the effect of rheological properties of the liquid towards effervescent atomization. They compared the resultant spray characteristics of water and a few mixtures of water, glycerol, and polyethylene oxide (PEO). The PEO solutions have different viscosity while maintaining a similar density to water. Acquired images portray similar disintegration to some stages of swirl atomization (dribble, distorted pencil, and fully developed spray), but with the addition of the following stages: the filaments with built-in droplets, the filaments with built-in bubbles, satellite bubbles, and bubbles connected by filaments. The observed added stages are shown in Fig. 26.

The disintegration of liquid in effervescent atomization is closely related to the breakup of bubbles. A study conducted by Cao and Macian-Juan [80] on the behaviour of bubbles in liquid jet breakup found that when the bubble radius becomes larger, the liquid jet velocity increases accordingly, and the cross section of the liquid jet becomes smaller. However, the larger bubbles take a longer time to break up. Gomez [81], Rahman et al. [82], Jagannathan et al. [83], Ghaemi [84], and Jobehdar [85] observed that the reduction of bubbles' size upon discharging from an effervescent atomizer resulted in a gradual reduction of droplet size. Roesler and Lefebvre [69] stated that for a bubble to break up liquid jet into fine droplets, it must possess enough energy. The bubble energy can be defined as:

$$E_b = RT\left(\frac{\dot{m}_G}{\dot{m}_L}\right) ln\left(\frac{P_G}{P_L}\right) \tag{14}$$

Linne et al. [86] classified disintegration regimes of effervescent atomization as mixed-mode breakup and rapid breakup. Mixed-mode breakup occurred at low liquid flowrates, characterized by the absence of jet spreading and rapid breakup, which is a common characteristic of effervescent sprays. Linne et al. [86] attributed that this behavior is probably caused by the failure of the flow to choke at the discharge orifice or because the value of Re is too low. Mixed-mode breakup involves the formation of large ligaments, which then further break up into droplets, even at very high GLR. The regimes of effervescent atomization proposed by Linne et al. [86] are shown in Fig. 27.

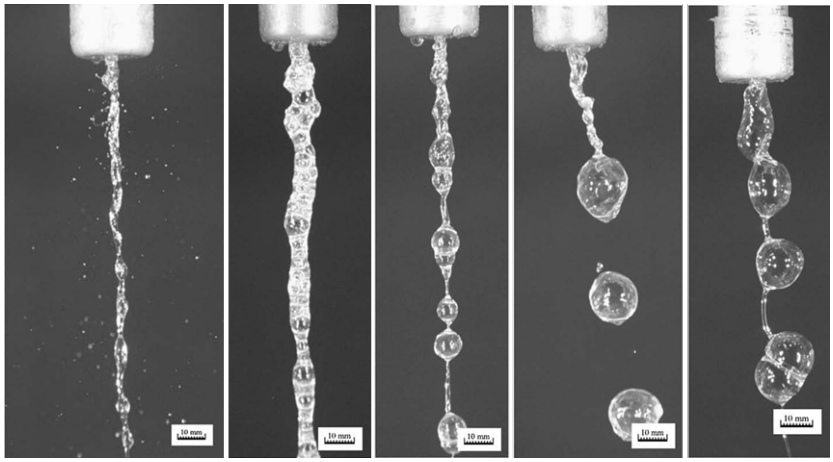

(a) **(b)** **(c)** **(d)** **(e)**

Fig. 26 *Added stages of effervescent spray disintegration. (a) filaments with built-in droplets, (b-c) the filaments with built-in bubbles, (d) satellite bubbles, and (e) bubbles connected by filaments. From Broniarz-Press et al. [79]*

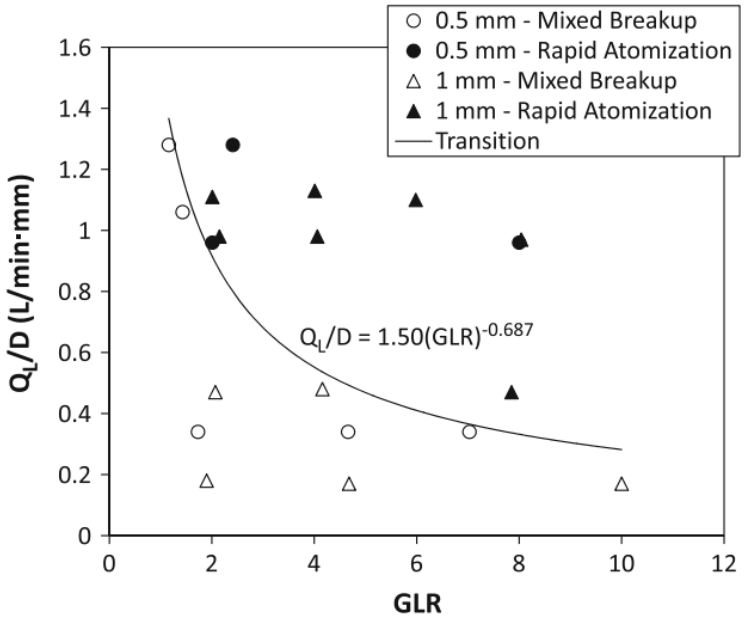

Fig. 27 *Regimes of liquid disintegration in effervescent atomization. From Linne et al. [86]*

A liquid disintegration regime map for effervescent atomization was proposed by Lorcher et al. [87]. They proposed a modification of Ohnesorge's liquid disintegration regimes map with the introduction of a critical mass flowrate plane, which turns the liquid disintegration regime map from two-dimensional to three-dimensional. To achieve critical flow conditions for this mixture, the individual phase flows cannot be varied independently from each other. Critical flow is only observed along a single curve in the described gray plane, as shown in Fig. 28. Details of the gray plane is shown in Fig. 29. The Reynolds numbers of liquid and gas with the constraint of the critical flow are given as:

$$Re_L = \frac{\dot{m}_{L,crit}\,(1-\dot{x})d_o}{\mu_L} \tag{15}$$

$$Re_G = \frac{\dot{m}_{L,crit}\cdot\dot{x}\cdot d_o}{\mu_G} \tag{16}$$

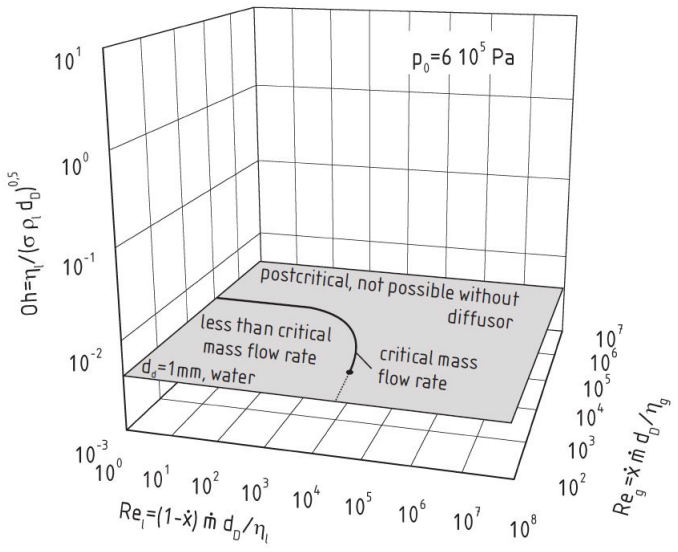

Fig. 28 *Regimes of liquid disintegration in effervescent atomization. From Lörcher et al. [87]*

Int. Journal of Integrated Engineering Vol. 17 No. 9 (2025) p. 85-116

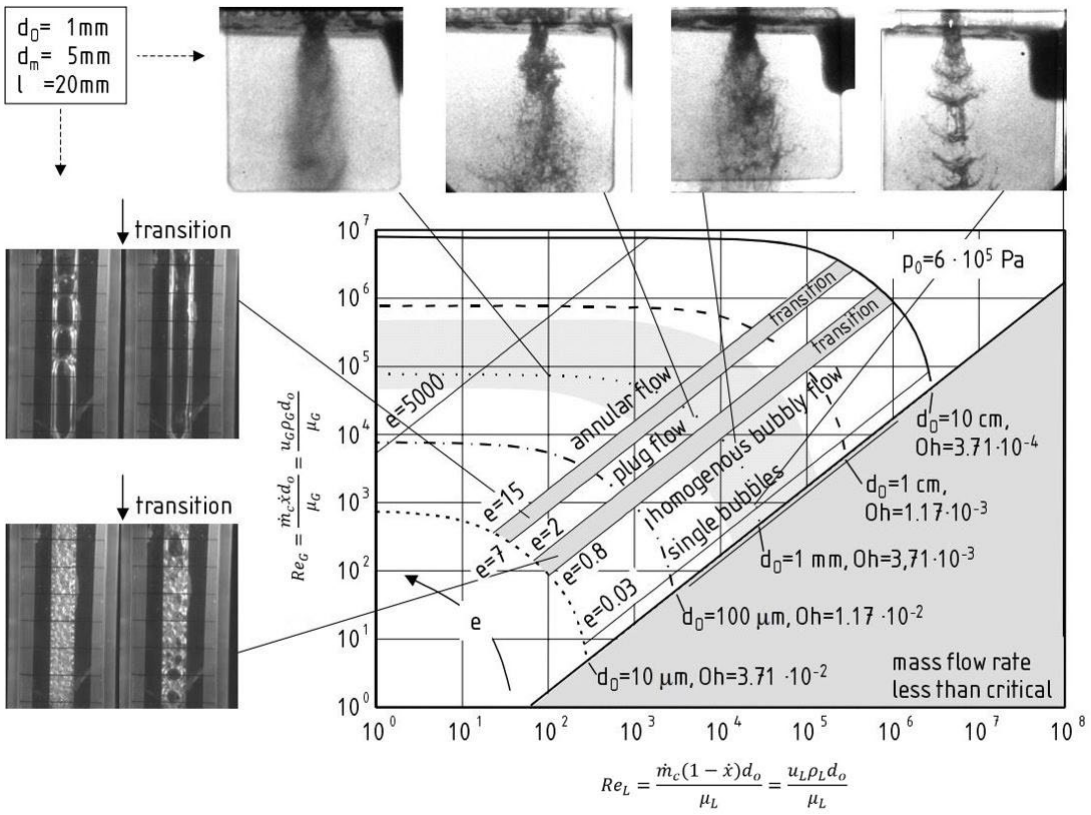

Fig. 29 *Details of gray plane in Fig. 29. From Lörcher et al. [87]*

Reynolds number is one of the most critical non-dimensional parameters in characterizing the liquid atomization. Reynolds number characterizes the primary atomization since primary atomization is initiated mainly by internal forces such as turbulence, inertial effects, or changes in velocity profile [2]. Stated before, effervescent atomization is classified as pneumatic atomization, i.e. an atomization that uses gas or vapour to assist the liquid atomization. Hence, affecting parameters to the effervescent atomization process dependent to both liquid and gas, i.e. liquid Reynolds number and gas Reynolds number.

4.1 Summary on Effervescent Atomization

Effervescent atomization introduces gas bubbles into the liquid upstream of the nozzle, shifting the breakup process into the interior of the nozzle. Liquid disintegration regimes of effervescent atomization comprise of bubbles trapped in liquid jet/sheet, bubble expansion, bubble bursting, formation of ligaments, and atomization. Bubble breakup is the primary source of disintegration regimes in effervescent. The size of bubbles inside the mixing chamber characterizes the resultant sprays discharging from the orifice. Reduction of bubble size resulted in a reduction of droplet size.

GLR is another factor that could shape the disintegration regime of effervescent atomization. Increase in GLR changes the internal flow regime from bubbly flow to slug flow and finally annular flow. The characteristics of the producing sprays depend on the flow regime which changes with GLR. However, Linne et al. [87] found that at low liquid flowrates, the effect of GLR on liquid disintegration is less significant.

5. Hypothesis for Liquid Disintegration Mechanism and Regimes of Swirl Effervescent Atomization

Swirl effervescent atomization is a combination of swirl atomization and effervescent atomization. Combining different mechanisms of liquid atomization in a single atomizer has been reported to be advantageous for each respective atomization. Kushari and Pandey [88] stated that combining two or more atomization mechanisms into a single atomizer could overcome the drawbacks of co-atomization. Although this type of atomizer has been applied in the combustion chamber of turbomachine [89], wide usage of this type of atomization is hampered by the insufficient knowledge on the fundamental mechanism.

Whitlow et al. [90] have conducted a study in characterizing effervescent atomizer with wide spray angle. Although geometrically, the studied atomizer does not involve swirling elements in producing a wide spray angle, the study was included in the analysis considering the enlargement of the spray angle by the atomizer. The result from Whitlow et al. [90] were replotted as a contour plot shown in Fig. 30. The plot was based on the liquid disintegration regime proposed by Lorcher et al. [87] as in Fig. 29. By inspection of the plot, the gas Reynolds number has a more prominent effect on the SMD than the liquid Reynolds number. The finest SMD is found at the highest gas Reynolds number, although the liquid Reynolds number is at the smallest value.

In contrast, the produced droplets tend to become coarser despite the increase in liquid Reynolds number. The contour plot visualizes a good resemblance with the liquid disintegration regime in Fig. 29 and may offer a good basis for hypothesizing the liquid disintegration regime of swirl effervescent atomization. The resemblance of the experimental result by Whitlow et al. [90] to the disintegration regime by Lorcher et al. [87] is strengthened with the replotting of the experimental result by Jedelsky and Jicha [91] as shown in Fig. 31. A similar trend is observed in Fig. 31, with gas Reynolds number remains the parameter in producing fine droplets regardless of the liquid Reynolds number.

Another finding that might be used as a basis to hypothesize liquid disintegration regime of swirl effervescent atomization is the acquired spray profiles images of swirl effervescent atomizer observed by Lee et al. [92]. The spray profile images shown in Fig. 32 present the spray profile images with the increase in GLR. The value of GLR (in percentage) starts with 0% at the top left to 1.0% at the bottom right. The spray profiles also depict likeliness to having the liquid disintegration regimes of swirl atomization portrays by the enlargement of spray angle with GLR. GLR has also been reported to slightly affecting the enlargement of the spray angle for effervescent atomizer by Hammad et al. [93]. This may suggest that GLR is an important parameter for both effervescent and swirl effervescent atomization. In general, GLR is directly proportional to gas Reynolds number.

Breakup length is also another parameter that may be used to hypothesize a disintegration regime. Typically, the spray angle and breakup length are the main characteristics of a swirl atomizer [94]. Breakup length is referred to as bubble bursting for effervescent-related atomizers. A study conducted by Ghaffar et al. [10] found that the length of a bubble bursting in swirl effervescent atomization is shorter compared to a bubble bursting of effervescent atomization observed by Gadgil and Raghunandan [71]. This was also observed by Lee et al. [92] in comparing the breakup length of two swirl effervescent atomizers with different spray angles. The occurrence of this phenomenon is due to the dependence of the liquid film on the liquid mass flowrate. Since the liquid mass flowrate was held at a constant value, the area of the liquid film remained unchanged. With the widening of the liquid film of the spray profile, the length of the liquid film tends to become shorter to maintain the liquid film's area. This has resulted in the spray having a shorter breakup length. This has also shown that the swirling element existed within the swirl effervescent atomization enhances the breakup of the liquid films. Fong et al. [95] showed that swirling not only modifies the transport of droplets in the spray cross-section but also enhances break-up and reduces the droplet mean diameter globally.

The proof of the hypotheses will be achieved via future works involving various areas of investigation which include:

- Characterizations of internal flow structures in the mixing chamber and discharge orifice.
- Visualizations of the spatial and temporal evolution of resulting sprays.
- Determination of significant factors affecting spray unsteadiness and possible solutions to reduce the unsteadiness.

Int. Journal of Integrated Engineering Vol. 17 No. 9 (2025) p. 85-116

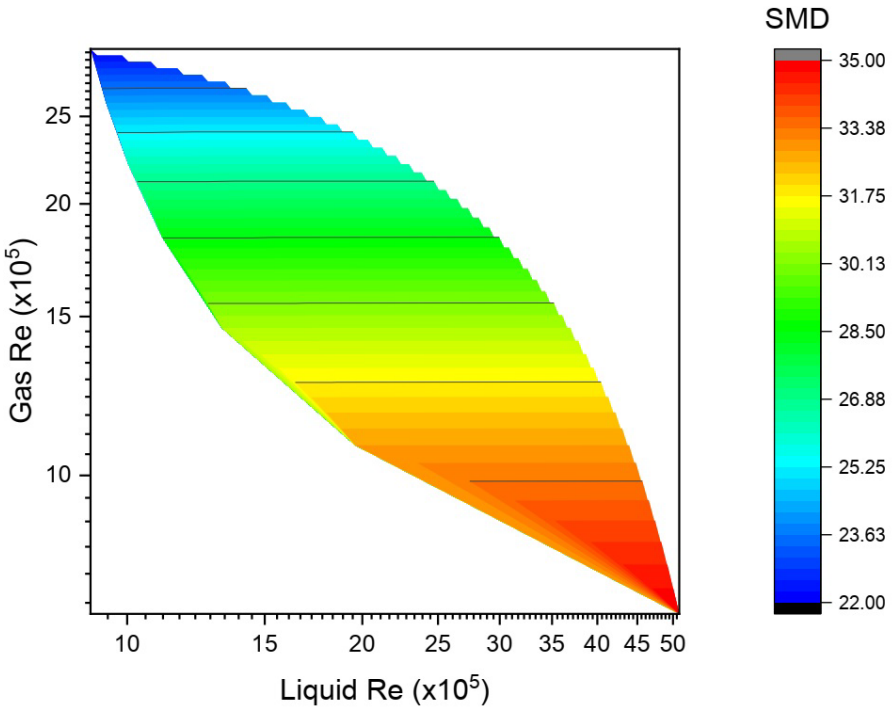

Fig. 30 *Replot experimental result by Whitlow et al. [90] as illustration to part of liquid disintegration regime map for effervescent atomization*

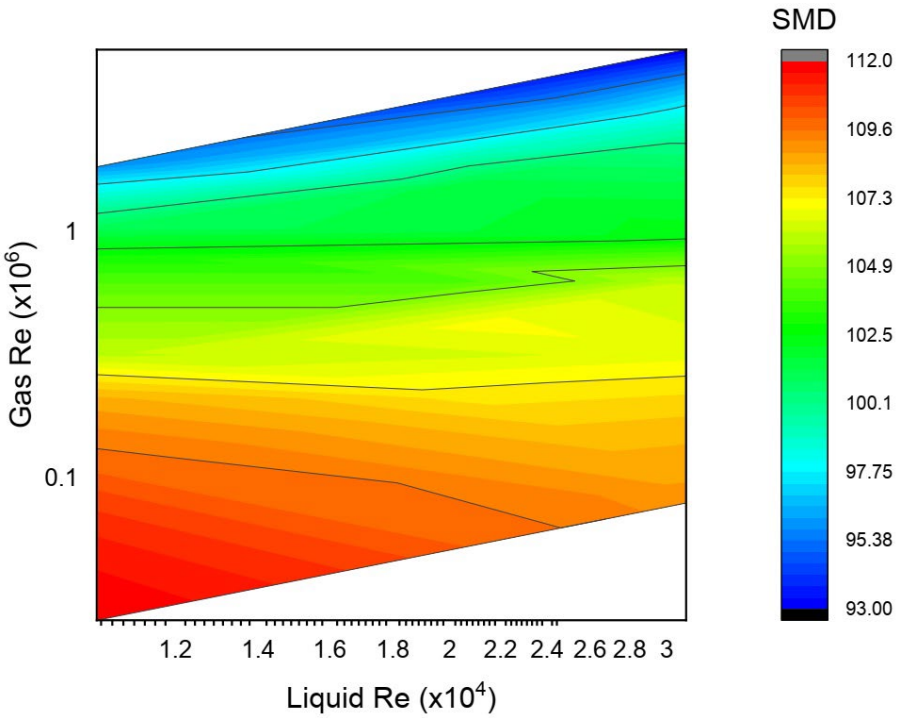

Fig. 31 *Replot of experimental result by Jedelsky and Jicha [91] as illustration to part of liquid disintegration regime map for effervescent atomization*

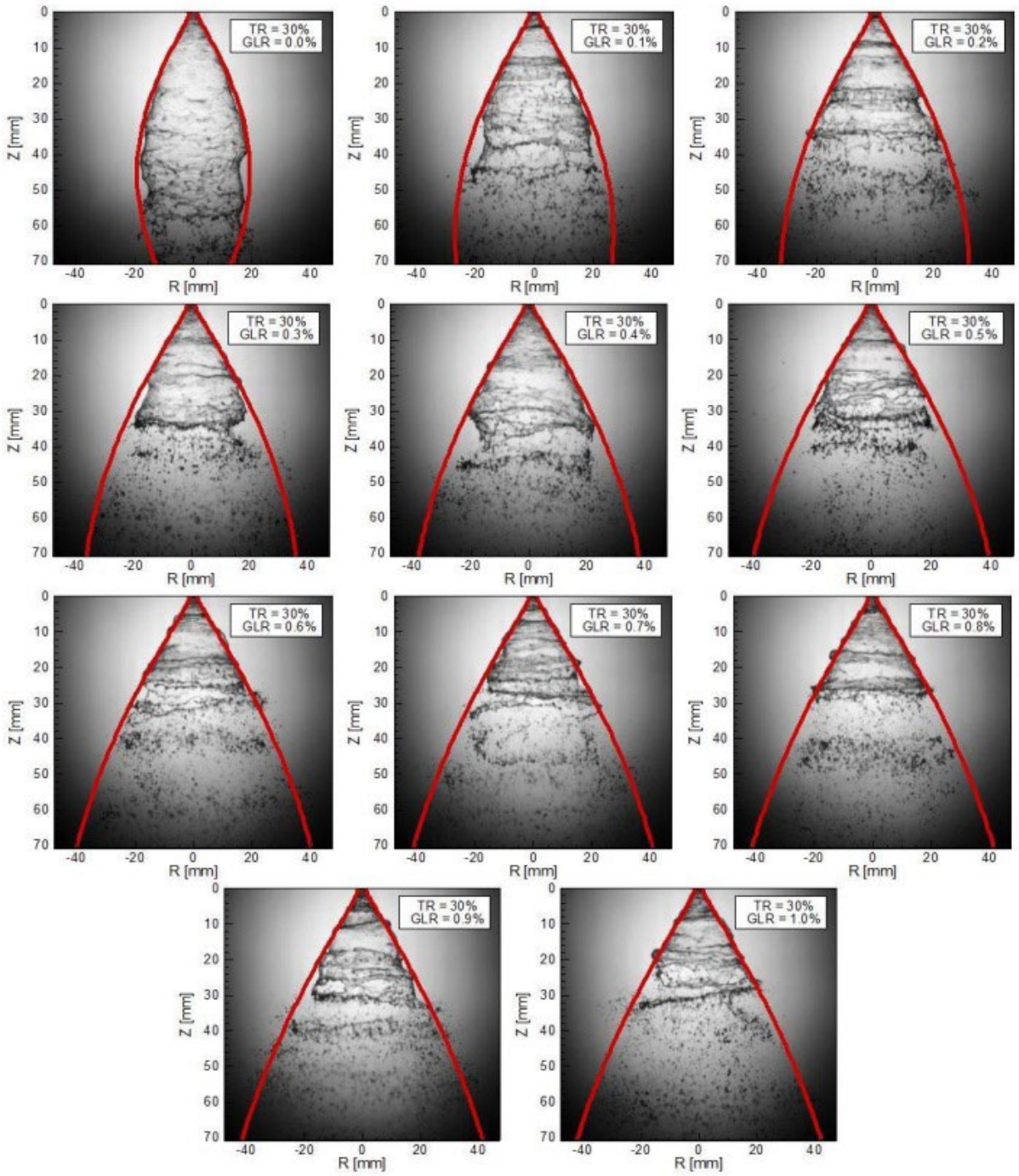

Fig. 32 *Spray profile images of swirl effervescent atomizer. From Lee et al. [92]*

6. Conclusions

This review has synthesized the liquid disintegration regimes of plain orifice, swirl, and effervescent atomizers, establishing a foundation to hypothesize the regime for swirl effervescent atomization. Plain orifice atomization progresses through regimes such as dripping, Rayleigh breakup, wind-induced instabilities, and fully developed sprays, commonly visualized via jet stability curves and Ohnesorge plots. Swirl atomization follows distinctive disintegration stages, i.e. dribble, distorted pencil, onion, tulip, and fully developed spray, where spray cone angle and SMD play critical roles. Effervescent atomization, driven by internal gas-liquid interactions, exhibits bubbly disintegration patterns, with GLR and bubble dynamics significantly shaping spray behaviour.

By integrating these understandings, swirl effervescent atomization is hypothesized to exhibit a hybrid regime, governed predominantly by gas Reynolds number or GLR. Experimental replots indicate strong correlations between finer droplet formation and higher gas Reynolds number, regardless of liquid Reynolds

number values. Moreover, swirling motion is shown to reduce breakup length and enhance spray dispersion as in swirl atomization, reinforcing its synergistic effect with internal gas bursting mechanisms.

Although promising, this hypothesis remains to be validated through future experimental and numerical investigations. These should explore internal flow fields, temporal spray evolution, and disintegration transitions under varying operating conditions. Ultimately, mapping the disintegration regime of swirl effervescent atomization not only enhances atomizer design flexibility but also unlocks its broader adoption in engineering applications where precise spray characteristics are critical.

Acknowledgement

This research was supported by the Ministry of Higher Education Malaysia through Fundamental Research Grant Scheme (FRGS), Reference number: FRGS/1/2019/TK03/UITM/02/14. This acknowledgment is also extended to the Research Management Center (RMC) of UiTM.

Conflict of Interest

Authors declare that there is no conflict of interest regarding the publication of the paper.

Author Contribution

The authors confirm contribution to the paper as follows: ***study conception and design:*** *Zulkifli Abdul Ghaffar, Salmiah Kasolang, Ahmad Hussein Abdul Hamid, Rolf D. Reitz;* ***data collection:*** *Zulkifli Abdul Ghaffar;* ***analysis and interpretation of results:*** *Zulkifli Abdul Ghaffar, Salmiah Kasolang, Ahmad Hussein Abdul Hamid, Rolf D. Reitz;* ***draft manuscript preparation:*** *Zulkifli Abdul Ghaffar. All authors reviewed the results and approved the final version of the manuscript.*

References

[1] V. Yang, M. Habiballah, J. Hulka, and M. Popp. (2004). *Liquid Rocket Thrust Chambers.* American Institute of Aeronautics and Astronautics. https://doi.org/10.2514/4.866760

[2] H. Liu. (2000). *Science and Engineering of Droplets: Fundamentals and Applications.* Noyes Publications.

[3] N. Ashgriz. (2011). Handbook of Atomization and Sprays. Springer US. https://doi.org/10.1007/978-1-4419-7264-4

[4] Ibrahim, A. (2006). Comprehensive study of internal flow field and linear and nonlinear instability of an annular liquid sheet emanating from an atomizer (Publication No. 3231127). [Doctoral dissertation, University of Cincinnati]. ProQuest Dissertations and Theses Global.

[5] ASTM International. (2012). *Standard E 1620-97: Standard Terminology Relating to Liquid Particles and Atomization.* ASTM International. https://www.astm.org/e1620-97r22.html

[6] Li, G., & Li, C. (2021). Experimental study on the spray steadiness of an internal-mixing twin-fluid atomizer. *Energy, 226,* 120394. https://doi.org/10.1016/j.energy.2021.120394

[7] Sovani, S. D., Sojka, P. E., & Lefebvre, A. H. (2001). Effervescent atomization. *Progress in energy and combustion science*, *27*(4), 483-521. https://doi.org/10.1016/S0360-1285(00)00029-0

[8] Shinjo, J., & Umemura, A. (2010). Simulation of liquid jet primary breakup: Dynamics of ligament and droplet formation. *International journal of multiphase Flow*, *36*(7), 513-532. https://doi.org/10.1016/j.ijmultiphaseflow.2010.03.008

[9] Ghaffar, Z. A., Kasolang, S., Hussein, A., Hamid, A., Ahmed, D. I., Sainan, K. I., & Nik Roselina, N. R. (2015). Gas core characteristics of swirl effervescent atomizer. *Jurnal Teknol*ogi, *76*, 58-62. https://doi.org/10.11113/jt.v76.5651

[10] Ghaffar, Z. A., Kasolang, S., Hamid, A. H. A., Ow, C. S., & Roselina, N. N. (2015). Design, development and performance evaluation of new swirl effervescent injector. *Jurnal Teknologi*, *75*(1). https://doi.org/10.11113/jt.v75.2813

[11] Ghaffar, Z. A., Kasolang, S., & Hamid, A. H. (2018). Spray Characteristics and Internal Flow Structures of Swirl Effervescent Atomizer. *International Journal of Engineering & Technology*, *7*(3.11), 58-61. https://doi.org/10.14419/ijet.v7i3.11.15930

[12] Ghaffar, Z. A., Kasolang, S., & Hamid, A. H. (2019, Dec 21 – 23). *Effect of Dimensionless Numbers on Spray Angle and Breakup Length of Swirl Effervescent Atomizer* [Conference session]. ILASS-Asia 2019, Ube, Japan. https://www.ilass-japan.gr.jp/_english/activity/ILASS-Asia2019/ILASS-Asia2019_program_final.pdf

[13] Ghaffar, Z. A., Kasolang, S., & Hamid, A. H. A. (2014). Characteristics of swirl effervescent atomizer spray angle. *Applied Mechanics and Materials*, *607*, 108-111. https://doi.org/10.4028/www.scientific.net/AMM.607.108

[14] Ghaffar, Z. A., Kasolang, S., Hamid, A. H. A., Sheng, O. C., & Bakar, M. A. A. (2015). Effect of geometrical parameters interaction on swirl effervescent atomizer spray angle. *Jurnal Teknologi*, *76*(9). https://doi.org/10.11113/jt.v76.5652

[15] Hamid, A. H. A., Ghaffar, Z. A., & Rus, N. C. (2018). Roles of Atomizing Gas in Swirl Effervescent Atomization. *International Journal of Engineering & Technology*, *7*(4.25), 24-28. https://doi.org/10.14419/ijet.v7i4.25.22242

[16] Ochowiak, M., Broniarz-Press, L., Rozanska, S., Matuszak, M., & Wlodarczak, S. (2015). Characteristics of spray angle for effervescent-swirl atomizers. *Chemical Engineering and Processing: Process Intensification*, *98*, 52-59. https://doi.rg/10.1016/j.cep.2015.10.008

[17] Ochowiak, M. (2016). Discharge coefficient of effervescent atomizers with the swirl motion phenomenon. *Experimental Thermal and Fluid Science*, *79*, 44-51. https://doi.org/10.1016/j.expthermflusci.2016.06.026

[18] Liu, L., Pei, N., Zhao, R., Tian, L., Duan, R., Zhang, Y., ... & Zhang, X. (2019). Effect of the two-phase hybrid mode of effervescent atomizer on the atomization characteristics. *Open Physics*, *17*(1), 960-965. https://doi.org/10.1515/phys-2019-0101

[19] Dumouchel, C. (2008). On the experimental investigation on primary atomization of liquid streams. *Experiments in fluids*, *45*, 371-422. https://doi.org/10.1007/s00348-008-0526-0

[20] Hede, P. D., Bach, P., & Jensen, A. D. (2008). Two-fluid spray atomisation and pneumatic nozzles for fluid bed coating/agglomeration purposes: A review. *Chemical Engineering Science*, *63*(14), 3821-3842. https://doi.org/10.1016/j.ces.2008.04.014

[21] Yao, S. (2013). Liquid Breakup and Atomization of Pressure Jet and Swirl Atomizers. [Doctoral dissertation, North Carolina State University]. NC State Repository.

[22] Lefebvre, A. H. and McDonell, V. G. (2017). *Atomization and Sprays, Second Edition*. CRC Press. https://www.routledge.com/Atomization-and-Sprays/Lefebvre-McDonell/p/book/9781498736251

[23] McCarthy, M. J., & Molloy, N. A. (1974). Review of stability of liquid jets and the influence of nozzle design. *The Chemical Engineering Journal*, *7*(1), 1-20. https://doi.org/10.1016/0300-9467(74)80021-3

[24] Bayvel, L. P. and Orzechowski, Z. (1993). *Liquid Atomization*. Taylor & Francis. https://www.routledge.com/Liquid-Atomization/Bayvel/p/book/9780891169598

[25] Zandian, A., Sirignano, W. A., & Hussain, F. (2017). Planar liquid jet: Early deformation and atomization cascades. *Physics of Fluids*, *29*(6). https://doi.org/10.1063/1.4986790

[26] Reitz, R. D. (1978). Atomization and Other Breakup Regimes of a Liquid Jet (Publication No. 7907964). [Doctoral dissertation, Princeton University]. ProQuest Dissertations and Theses Global.

[27] No, S. Y., Ryu, K. Y., Rhim, J. H., & Lim, S. B. (1999). Prediction of Critical Reynolds Number in Stability Curve of Liquid Jet (I). *Journal of ILASS-Korea*, *4*(1), 55-61.

[28] S. B. Lim, J. D. So, and S. Y. No, "Prediction of Critical Reynolds Number in Stability Curve of Liquid Jet (II)," J. ILASS Korea, vol. 4, no. 2, pp. 47–52, 1999.

[29] Van de Sande, E., & Smith, J. M. (1976). Jet break-up and air entrainment by low velocity turbulent water jets. *Chemical Engineering Science*, *31*(3), 219-224. https://doi.org/10.1016/0009-2509(76)85060-9

[30] Bravo, L., Kim, D., Ham, F., Powell, C., & Kastengren, A. (2019). Effects of fuel viscosity on the primary breakup dynamics of a high-speed liquid jet with comparison to X-ray radiography. *Proceedings of the Combustion Institute*, *37*(3), 3245-3253. https://doi.org/10.1016/j.proci.2018.05.064

[31] Khavkin, Y. I. (2004). *Theory and practice of swirl atomizers*. Taylor & Francis.

[32] Khodayari, H., Ommi, F., & Saboohi, Z. (2018). Investigation of the primary breakup length and instability of non-Newtonian viscoelastic liquid jets. *The International Journal of Multiphysics*, *12*(4), 327-348. https://doi.org/10.21152/1750-9548.12.4.327

[33] Sallam, K. A., Dai, Z., & Faeth, G. M. (2002). Liquid breakup at the surface of turbulent round liquid jets in still gases. *International Journal of Multiphase Flow*, *28*(3), 427-449. https://doi.org/10.1016/S0301-9322(01)00067-2

[34] Pan, Y., & Suga, K. (2006). A numerical study on the breakup process of laminar liquid jets into a gas. *Physics of fluids*, *18*(5). https://doi.org/10.1063/1.2194936

[35] Etzold, M., Deswal, A., Chen, L., & Durst, F. (2018). Break-up length of liquid jets produced by short nozzles. *International Journal of Multiphase Flow*, *99*, 397-407. https://doi.org/10.1016/j.ijmultiphaseflow.2017.11.006

[36] Sterling, A. M., & Sleicher, C. A. (1975). The instability of capillary jets. *Journal of Fluid Mechanics*, *68*(3), 477-495. https://doi.org/10.1017/S0022112075001772

[37] Arai, M., Tabata, M., Hiroyasu, H., & Shimizu, M. (1984). Disintegrating process and spray characterization of fuel jet injected by a diesel nozzle. *SAE transactions*, 358-371. https://doi.org/10.4271/840275

[38] He, X., Chen, C., Yang, Y., & Yan, Z. (2020). Experimental study on the flow field distribution characteristics of an open-end swirl injector under ambient pressure. *Aerospace Science and Technology*, *98*, 105691. https://doi.org/10.1016/j.ast.2020.105691

[39] Fu, Q. F., & Yang, L. J. (2015). Visualization studies of the spray from swirl injectors under elevated ambient pressure. *Aerospace Science and Technology*, *47*, 154-163. https://doi.org/10.1016/j.ast.2015.09.027

[40] Leroux, S., Dumouchel, C., & Ledoux, M. (1996). The stability curve of Newtonian liquid jets. *Atomization and sprays*, *6*(6). https://doi.org/10.1615/AtomizSpr.v6.i6.10

[41] Yang, L. J., Qu, Y. Y., Fu, Q. F., Xu, B. R., Zhang, W., & Du, M. L. (2013). Linear stability analysis of a slightly viscoelastic liquid jet. *Aerospace Science and Technology*, *28*(1), 249-256. https://doi.org/10.1016/j.ast.2012.11.005

[42] Zhang, Z., & Shin, D. H. (2020). Effect of ambient pressure oscillation on the primary breakup of cylindrical liquid jet spray. *International Journal of Spray and Combustion Dynamics*, *12*, 1756827720935553. https://doi.org/10.1177/1756827720935553

[43] Spangler, C. A., Hilbing, J. H., & Heister, S. D. (1995). Nonlinear modeling of jet atomization in the wind-induced regime. *Physics of Fluids*, *7*(5), 964-971. https://doi.org/10.1063/1.868572

[44] Ohnesorge, W. V. (1936). Die bildung von tropfen an düsen und die auflösung flüssiger strahlen [Formation of drops by nozzles and the breakup of liquid jets]. *ZAMM-Journal of Applied Mathematics and Mechanics/Zeitschrift für Angewandte Mathematik und Mechanik*, *16*(6), 355-358. https://doi.org/10.1002/zamm.19360160611

[45] Hilbing, J. H., & Heister, S. D. (1996). Droplet size control in liquid jet breakup. *Physics of Fluids*, *8*(6), 1574-1581. https://doi.org/10.1063/1.868931

[46] Wang, F., & Fang, T. (2015). Liquid jet breakup for non-circular orifices under low pressures. *International Journal of Multiphase Flow*, *72*, 248-262. https://doi.org/10.1016/j.ijmultiphaseflow.2015.02.015

[47] Fung, M. C., Inthanvong, K., Yang, W., & Tu, J. (2012). Experimental and numerical modelling of nasal spray atomisation. In C.B. Solnordal, P. Liovic, G.W. Delaney and P.J. Witt (Eds.), 9*th International Conference on CFD in The Minerals and Process Industries* (pp. 1-6). CSIRO. http://hdl.handle.net/102.100.100/98506?index=1

[48] Dafsari, R. A., Lee, H. J., Han, J., Park, D. C., & Lee, J. (2019). Viscosity effect on the pressure swirl atomization of an alternative aviation fuel. *Fuel*, *240*, 179-191. https://doi.org/10.1016/j.fuel.2018.11.132

[49] Laurila, E., Roenby, J., Maakala, V., Peltonen, P., Kahila, H., & Vuorinen, V. (2019). Analysis of viscous fluid flow in a pressure-swirl atomizer using large-eddy simulation. *International Journal of Multiphase Flow*, *113*, 371-388. https://doi.org/10.1016/j.ijmultiphaseflow.2018.10.008

[50] Park, B. S., Kim, H. Y., & Kim, Y. Effects of Fuel Temperature on the Spray Characteristics of a Dual-orifice Type Swirl Injector. In R. Ragucci (Eds.), *9th International Conference on Liquid Atomization and Spray Systems* (pp. 1704). ILASS Europe.

[51] Yan, K., Ning, Z., Lü, M., Sun, C., Fu, J., & Li, Y. (2015). Spatial instability in annular swirling viscous liquid sheet. *Physics of Fluids*, *27*(2). https://doi.org/10.1063/1.4906986

[52] Yao, S., Zhang, J., & Fang, T. (2012). Effect of viscosities on structure and instability of sprays from a swirl atomizer. *Experimental Thermal and Fluid Science*, *39*, 158-166. https://doi.org/10.1016/j.expthermflusci.2012.01.020

[53] Rhim, J. H., & No, S. Y. (2001). Breakup length of conical emulsion sheet discharged by pressure-swirl atomizer. *International Journal of Automotive Technology*, *2*(3), 103-107.

[54] Kang, Z., Wang, Z. G., Li, Q., & Cheng, P. (2018). Review on pressure swirl injector in liquid rocket engine. *Acta Astronautica*, *145*, 174-198. https://doi.org/10.1016/j.actaastro.2017.12.038

[55] Prakash, R. S., Gadgil, H., & Raghunandan, B. N. (2014). Breakup processes of pressure swirl spray in gaseous cross-flow. *International Journal of Multiphase Flow*, *66*, 79-91. https://doi.org/10.1016/j.ijmultiphaseflow.2014.07.002

[56] Ghorbanian, K., Ashjaee, M., Soltani, M., Mesbahi, M., & Morad, M. (2003). Experimental flow visualization of single swirl spray pattern at various pressure drops. In AIAA (Eds.), *39th AIAA/ASME/SAE/ASEE Joint Propulsion Conference and Exhibit* (pp. 4758). American Institute of Aeronautics and Astronautics, Inc. https://doi.org/10.2514/6.2003-4758

[57] Ramamurthi, K., & Tharakan, T. J. (1998). Flow transition in swirled liquid sheets. *AIAA journal*, *36*(3), 420-427. https://doi.org/10.2514/2.380

[58] Sindayihebura, D., & Dumouchel, C. (2001). 3. Pressure atomiser: Hole breakup of the sheet. *Journal of Visualization*, *4*(1), 5-5. https://doi.org/10.1007/bf03182447

[59] Loustalan, P. W., Davy, M. H., & Williams, P. A. (2003). Experimental investigation into the liquid sheet break-up of high-pressure DISI swirl atomizers. *SAE Technical Paper*, 2003-01-3102. https://doi.org/10.4271/2003-01-3102

[60] Najafi, S. M. A., Mikaniki, P., & Ghassemi, H. (2020). Microscopic and macroscopic atomization characteristics of a pressure-swirl atomizer, injecting a viscous fuel oil. *Chinese Journal of Chemical Engineering*, *28*(1), 9-22. https://doi.org/10.1016/j.cjche.2019.04.006

[61] Wang, X. F., & Lefebvre, A. H. (1987). Mean drop sizes from pressure-swirl nozzles. *Journal of Propulsion and Power*, *3*(1), 11-18. https://doi.org/10.2514/3.22946

[62] Jasuja, A. (1979). Atomization of Crude and Residual Fuel Oils. *Journal of Engineering for Power*, *101*(2), 250-258. https://doi.org/10.1115/1.3446480

[63] Rashad, M., Yong, H., & Zekun, Z. (2016). Effect of geometric parameters on spray characteristics of pressure swirl atomizers. *International Journal of Hydrogen Energy*, *41*(35), 15790-15799. https://doi.org/10.1016/j.ijhydene.2016.04.037

[64] Vijay, G. A., Moorthi, N. S. V., & Manivannan, A. (2015). Internal and external flow characteristics of swirl atomizers: a review. *Atomization and Sprays*, *25*(2). https://doi.org/10.1615/AtomizSpr.2014010219

[65] Halder, M. R., Dash, S. K., & Som, S. K. (2002). Initiation of air core in a simplex nozzle and the effects of operating and geometrical parameters on its shape and size. *Experimental Thermal and Fluid Science*, *26*(8), 871-878. https://doi.org/10.1016/S0894-1777(02)00153-X

[66] Lee, E. J., Oh, S. Y., Kim, H. Y., James, S. C., & Yoon, S. S. (2010). Measuring air core characteristics of a pressure-swirl atomizer via a transparent acrylic nozzle at various Reynolds numbers. *Experimental Thermal and Fluid Science*, *34*(8), 1475-1483. https://doi.org/10.1016/j.expthermflusci.2010.07.010

[67] Kim, D., Im, J. H., Koh, H., & Yoon, Y. (2007). Effect of ambient gas density on spray characteristics of swirling liquid sheets. *Journal of Propulsion and Power*, *23*(3), 603-611. https://doi.org/10.2514/1.20161

[68] Lefebvre, A. (1988). A novel method of atomization with potential gas turbine applications. *Defense Science Journal*, *38*(4), 353-362.

[69] Roesler, T. C., & Lefebvre, A. H. (1989). Studies on aerated-liquid atomization. *International Journal of Turbo and Jet Engines*, *6*(3-4), 221-230. https://doi.org/10.1515/TJJ.1989.6.3-4.221

[70] Lefebvre, A. H., Wang, X. F., & Martin, C. A. (1988). Spray characteristics of aerated-liquid pressure atomizers. *Journal of Propulsion and Power*, *4*(4), 293-298. https://doi.org/10.2514/3.23066

[71] Gadgil, H. P., & Raghunandan, B. N. (2011). Some features of spray breakup in effervescent atomizers. *Experiments in Fluids*, *50*, 329-338. https://doi.org/10.1007/s00348-010-0929-6

[72] Santangelo, P. J., & Sojka, P. E. (1994). Focused-image holography as a dense-spray diagnostic. *Applied Optics*, *33*(19), 4132-4136. https://doi.org/10.1364/AO.33.004132

[73] Ghaffar, Z. A., Hamid, A. H. A., & Rashid, M. S. F. M. (2012, June). A review on spray characteristics of effervescent atomizer under various geometrical parameters and operating condition. *AIP Conference Proceedings, 1440*(1), 586-590. https://doi.org/10.1063/1.4704266

[74] Ghaffar, Z. A., Hamid, A. H. A., & Rashid, M. S. F. M. (2012). Spray Characteristics of Swirl Effervescent Injector in Rocket Application: A Review. *Applied Mechanics and Materials*, *225*, 423-428. https://doi.org/10.4028/www.scientific.net/AMM.225.423

[75] Chen, C., Gong, X., Wang, Y., & He, X. (2024). The Effect of Ambient Pressure and Gas–Liquid Ratio on the Spray Characteristics of an Effervescent Atomizer. *International Journal of Aeronautical and Space Sciences*, *25*(1), 154-163. https://doi.org/10.1007/s42405-023-00638-9

[76] Zaremba, M., Weiß, L., Malý, M., Wensing, M., Jedelský, J., & Jícha, M. (2017). Low-pressure twin-fluid atomization: Effect of mixing process on spray formation. *International Journal of Multiphase Flow*, *89*, 277-289. https://doi.org/10.1016/j.ijmultiphaseflow.2016.10.015

[77] Mlkvik, M., Stähle, P., Schuchmann, H. P., Gaukel, V., Jedelsky, J., & Jicha, M. (2015). Twin-fluid atomization of viscous liquids: The effect of atomizer construction on breakup process, spray stability and droplet size. *International Journal of Multiphase Flow*, *77*, 19-31. https://doi.org/10.1016/j.ijmultiphaseflow.2015.06.010

[78] Zaremba, M., Kozák, J., Malý, M., Weiß, L., Rudolf, P., Jedelský, J., & Jícha, M. (2018). An experimental analysis of the spraying processes in improved design of effervescent atomizer. *International Journal of Multiphase Flow*, *103*, 1-15. https://doi.org/10.1016/j.ijmultiphaseflow.2018.01.012

[79] Broniarz-Press, L., Ochowiak, M., & Woziwodzki, S. (2010). Atomization of PEO aqueous solutions in effervescent atomizers. *International Journal of Heat and Fluid Flow*, *31*(4), 651-658. https://doi.org/10.1016/j.ijheatfluidflow.2010.02.005

[80] Cao, Y., & Macián-Juan, R. (2020). Numerical investigation of central breakup of large bubble induced by liquid jet. *Physics of Fluids*, *32*(3). https://doi.org/10.1063/1.5144975

[81] Gomez, J. 2010. Influence of bubble size on an effervescent atomization. [Doctoral dissertation, University of Alberta]. Education & Research Archive, University of Alberta Library.

[82] Rahman, M. A., Balzan, M., Heidrick, T., & Fleck, B. A. (2012). Effects of the gas phase molecular weight and bubble size on effervescent atomization. *International Journal of Multiphase Flow*, *38*(1), 35-52. https://doi.org/10.1016/j.ijmultiphaseflow.2011.08.013

[83] Jagannathan, T. K., Nagarajan, R., & Ramamurthi, K. (2011). Effect of ultrasound on bubble breakup within the mixing chamber of an effervescent atomizer. *Chemical Engineering and Processing: Process Intensification*, *50*(3), 305-315. https://doi.org/10.1016/j.cep.2011.01.006

[84] Ghaemi, S. (2009). Investigation of effervescent atomization using laser-based measurement techniques. [Master of Science dissertation, University of Alberta]. Education & Research Archive, University of Alberta Library.

[85] Jobehdar, M. H. (2014). Experimental Study of Two-Phase Flow in a Liquid Cross-Flow and an Effervescent Atomizer (Publication No. 29242471). [Doctoral dissertation, The University of Western Ontario]. ProQuest Dissertations and Theses Global.

[86] Linne, M., Sedarsky, D., Meyer, T., Gord, J., & Carter, C. (2010). Ballistic imaging in the near-field of an effervescent spray. *Experiments in Fluids*, *49*, 911-923. https://doi.org/10.1007/s00348-010-0883-3

[87] Lorcher, M., Schmidt, F., & Mewes, D. (2005). Effervescent atomization of liquids. *Atomization and Sprays*, *15*(2). https://doi.org/10.1615/AtomizSpr.v15.i2.30

[88] Kushari, A., & Pandey, S. (2008). A Controllable Twin-Fluid Internally Mixed Swirl Atomizer. *Recent Patents on Mechanical Engineering*, *1*(1), 45-50.

[89] Furletov, V. I., Noel, T. O. M., Rollin, G. L., Vasilev, A. J., & Yagodkin, V. I. (2009). *Effervescence injector for an aero-mechanical system for injecting air/fuel mixture into a turbomachine combustion chamber.* (U.S. Patent No. 7,568,345). U.S. Patent and Trademark Office. https://patents.google.com/patent/US7568345B2/en

[90] Whitlow, J. D., Lefebvre, A. H., & Rollbuhler, R. J. (1993). Experimental studies on effervescent atomizers with wide spray angles. *In* AGARD (Eds.), AGARD Meeting on 'Fuels and Combustion Technology for Advanced Aircraft Engines (pp. 38.1-38.11). Advisory Group for Aerospace Research & Development (AGARD).

[91] Jedelsky, J., & Jicha, M. (2010). Novel modifications of twin-fluid atomizers: performance, advantages, and drawbacks. In M. Jicha (Eds.), *23rd Annual Conference on Liquid Atomization and Spray Systems – ILASS Europe 2010,* (pp. 203.1-203.5). ILASS Europe. https://www.ilasseurope.org/ICLASS/ilass2010/FILES/FULL_PAPERS/203.pdf

[92] Lee, W., Hwang, D., Ahn, K., & Yoon, Y. (2019). Spray Characteristics of Effervescent Swirl Injectors for Variable Thrust. *Journal of the Korean Society of Propulsion Engineers*, *23*(2), 1-12. https://doi.org/10.6108/kspe.2019.23.2.001

[93] Hammad, F. A., Sun, K., Che, Z., Jedelsky, J., & Wang, T. (2021). Internal two-phase flow and spray characteristics of outside-in-liquid twin-fluid atomizers. *Applied Thermal Engineering*, *187*, 116555. https://doi.org/10.1016/j.applthermaleng.2021.116555

[94] Jeong, S., & Yoon, Y. (2021). Sheet-breakup characteristics of a closed-type swirl injector considering internal flow instability. *Acta Astronautica*, *186*, 363-371. https://doi.org/10.1016/j.actaastro.2021.05.049

[95] Fong, K. O., Xue, X., Osuna-Orozco, R., & Aliseda, A. (2024). Gas-liquid coaxial atomization with swirl in high-pressure environments. *International Journal of Multiphase Flow*, 104767. https://doi.org/10.1016/j.ijmultiphaseflow.2024.104767